Genetic Underpinnings of Risky Behavior Relate to Altered Neuroanatomy

One Sentence Summary: Risky behavior and its genetic associations are linked to lower grey matter volume in distinct brain regions.

G. Aydogan[1], R. Daviet[2], R. Karlsson Linnér[3], T. A. Hare[1], J. W. Kable[2,4], H. R. Kranzler[5,6], R. R. Wetherill[5], C. C. Ruff[1], P. D. Koellinger[3], G. Nave[2]

[1]Zurich Center for Neuroeconomics (ZNE), Department of Economics, University of Zurich, Zurich, Switzerland.

[2]Marketing Department, The Wharton School, University of Pennsylvania, Philadelphia, PA, USA

[3]Department of Economics, School of Business and Economics, Vrije Universiteit Amsterdam, Amsterdam, the Netherlands

[4]Department of Psychology, University of Pennsylvania, Philadelphia, PA, USA

[5]Department of Psychiatry, University of Pennsylvania Perelman School of Medicine, Philadelphia, PA, USA

[6]Veterans Integrated Service Network 4, Mental Illness Research, Education and Clinical Center, Crescenz Veterans Affairs Medical Center, Philadelphia, PA, USA

Abstract:

Previous research points to the heritability of risk-taking behavior. However, evidence on how genetic dispositions are translated into risky behavior is scarce. Here, we report a genetically-informed neuroimaging study of real-world risky behavior in a large European sample (*N*=12,675). We found negative associations between risky behavior and grey matter volume (GMV) in distinct brain regions, including amygdala, ventral striatum, hypothalamus and dorsolateral prefrontal cortex (dlPFC). Polygenic risk scores for risky behaviors, derived from a genome-wide association study in an independent sample (*N*=297,025), were inversely associated with GMV in dlPFC, putamen, and hypothalamus. This relation mediated ~2.2% of the association between genes and behavior. Our results highlight distinct heritable neuroanatomical features as manifestations of the genetic propensity for risk taking.

Taking risks—an essential element of many human experiences and achievements—requires balancing uncertain positive and negative outcomes. For instance, exploration, innovation and entrepreneurship can yield great benefits, but are also prone to failure (*1*). Conversely, excessive risk-taking in markets can have enormous societal costs, such as speculative price bubbles (*2*). Similarly, common behaviors such as *smoking, drinking, sexual promiscuity,* or *speeding* are considered rewarding by many, but might expose individuals and their environment to deleterious health and financial consequences. In 2010, the combined economic burden in the United States of these risky behaviors was estimated to be about $593.3 billion (*3*–*6*). Although previous findings point to the partial heritability of risk tolerance and risky behaviors (*7*) and neuroanatomical measures exhibit high heritability (*8*, *9*), little is known about the brain features involved in translating genetic dispositions into risky behavioral phenotypes (*8*).

Recent research using structural brain-imaging data from small, non-representative samples (comprising up to a few hundred participants) point to several neuroanatomical associations with risk tolerance (*10*–*12*). However, this literature is limited by the studies' low statistical power (*13*), and generalizability of their findings to other populations is questionable. Small sample sizes have also limited the ability to control systematically for many factors that could confound observed relations between brain features and risky behavior, such as height (*14*) and genetic population structure (*15*). Moreover, despite evidence that the effects of genetic factors are likely mediated by their influence on the brain and its development (*7*, *16*), neuroscientific and genetic approaches to understanding the biology of risky behavior have largely proceeded in

isolation – perhaps due to the lack of large study samples that include both genetic and brain imaging measures.

Here, we utilize data obtained in a prospective epidemiological study of ~500,000 individuals aged 40 to 69 years [the UK Biobank (UKB (*8*)] to carry out a pre-registered investigation [https://osf.io/qkp4g/, see Supplementary Online Materials (SOM) for deviations from the analysis plan] of the relationship between individual differences in brain anatomy and the propensity to engage in risky behavior across four domains. To investigate how these neuroanatomical endophenotypes mediate the influence of the genetic associations on the behavioral phenotype, we isolate specific differences in brain anatomy that link genetic predispositions with risky behavior by deriving polygenic risk scores (PRS) from a genome-wide association study (GWAS) in an independent sample (N = 297,025).

Grey Matter Volume Associations with Risky Behavior

Akin to a previous investigation (*7*), we constructed a measure of risky behavior by extracting the first principal component from four self-reported measures of drinking, smoking, speeding on motorways and sexual promiscuity (N = 315,855; see Fig 1A and SOM Fig S1-S2 for descriptive statistics). This measure of risky behavior exhibits a genetic correlation with many outcomes, including cannabis use (r_g = 0.72, SE = 0.02), general risk tolerance (r_g = 0.56, SE = 0.02), self-employment (r_g = 0.52; SE = 0.30), suicide attempt (r_g = 0.47, SE = 0.07), antisocial behavior (r_g = 0.45, SE = 0.14), extraversion (r_g = 0.34, SE = 0.04), and age at first sexual experience (r_g = -0.54, SE = 0.02) (SOM Table S1). Thus, our measure captures a broad range of relevant events and behaviors. We first regressed our measure of risky behavior on total (whole-brain) grey

matter volume (GMV), while controlling for age, birth year, gender, handedness, height, total intracranial volume and the first 40 genetic principal components, which account for genetic population structure (see SOM). To exclude confounding effects of excessive alcohol consumption, we excluded from the analysis all current or former heavy drinkers (see SOM) (*17*). Our results revealed an inverse association between total GMV and risky behavior (standardized $\beta = -.122$; 95% confidence interval (CI) [−.156, −.087]; $P < 4.86 \times 10^{-12}$).

To identify specific brain regions related to risky behavior, we performed a whole-brain voxel-based morphometry (VBM) analysis that regressed our measure of risky behavior separately on GMV in each voxel across the brain, adjusting for the same control variables. We identified localized inverse associations between risky behavior and GMV in distinct regions, only some of which were expected based on previous small-scale studies (see Fig. 1B, Fig. S3 and Table S2). In subcortical areas, we identified associations bilaterally in the amygdala and ventral striatum (VS), as well as in less-expected areas such as the posterior hippocampus, putamen, thalamus, hypothalamus, and cerebellum. We also identified bilateral associations between risky behavior and GMV in cortical regions including the ventral medial prefrontal cortex (vmPFC), dorsolateral prefrontal cortex (dlPFC), ventro-anterior insula (aINS) and the precentral gyrus. In all of these regions, GMV was negatively associated with the propensity to engage in risky behaviors. We found no positive associations between GMV and risky behavior across the brain.

To quantify effect sizes of the associations between risky behavior and GMV in anatomically-defined brain structures, we conducted a follow-up analysis at the region

of interest (ROI) level. This analysis primarily relied on the imaging-derived phenotypes (IDPs) provided by the UKB brain imaging processing pipeline (*8*), which used parcellations from the Harvard-Oxford cortical and subcortical atlases and the Diedrichsen cerebellar atlas. We derived additional IDPs using unbiased masks based on the results of the voxel-level analysis (see SOM). This analysis identified negative associations between risky behavior and GMV in 23 anatomical structures, with standardized βs between −0.079 and −0.036 (Fig. 1C and Fig. S4), the largest of which was in the right ventro-aINS; (β = −0.079; 95% CI [−.103, −.055]; P_{uncorr} = 1.34 × 10^{-10}).

We found similar results in robustness checks that controlled for the linear effect of alcohol (see Fig. S5).

Overlap between Grey Matter Volume Differences and fMRI Meta-Analysis

To investigate whether the neuroanatomical associations of real-world risky behavior correspond to localized activation patterns identified in fMRI studies of risky decision-making, we conducted a conjunction analysis that compared our VBM results with data obtained from a publicly available meta-analysis of fMRI studies on risky behavior (*18*) (N = 4,717 participants, K = 101 individual studies, see Table S3). The analysis revealed several brain regions whose anatomical associations with risky behavior converged with functional engagement during risky decision-making, including the thalamus, amygdala, vmPFC, and dlPFC (Fig 1D).

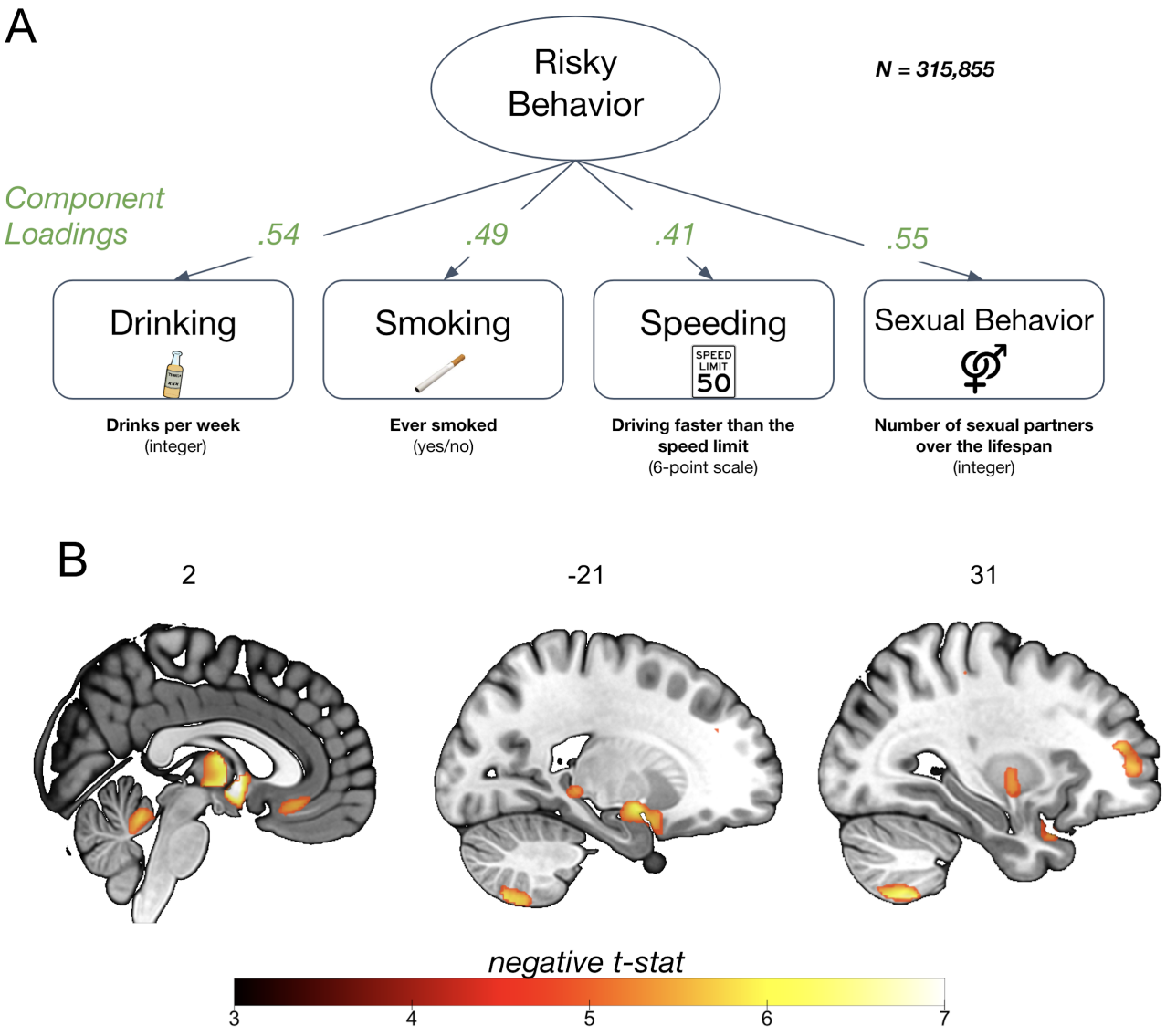

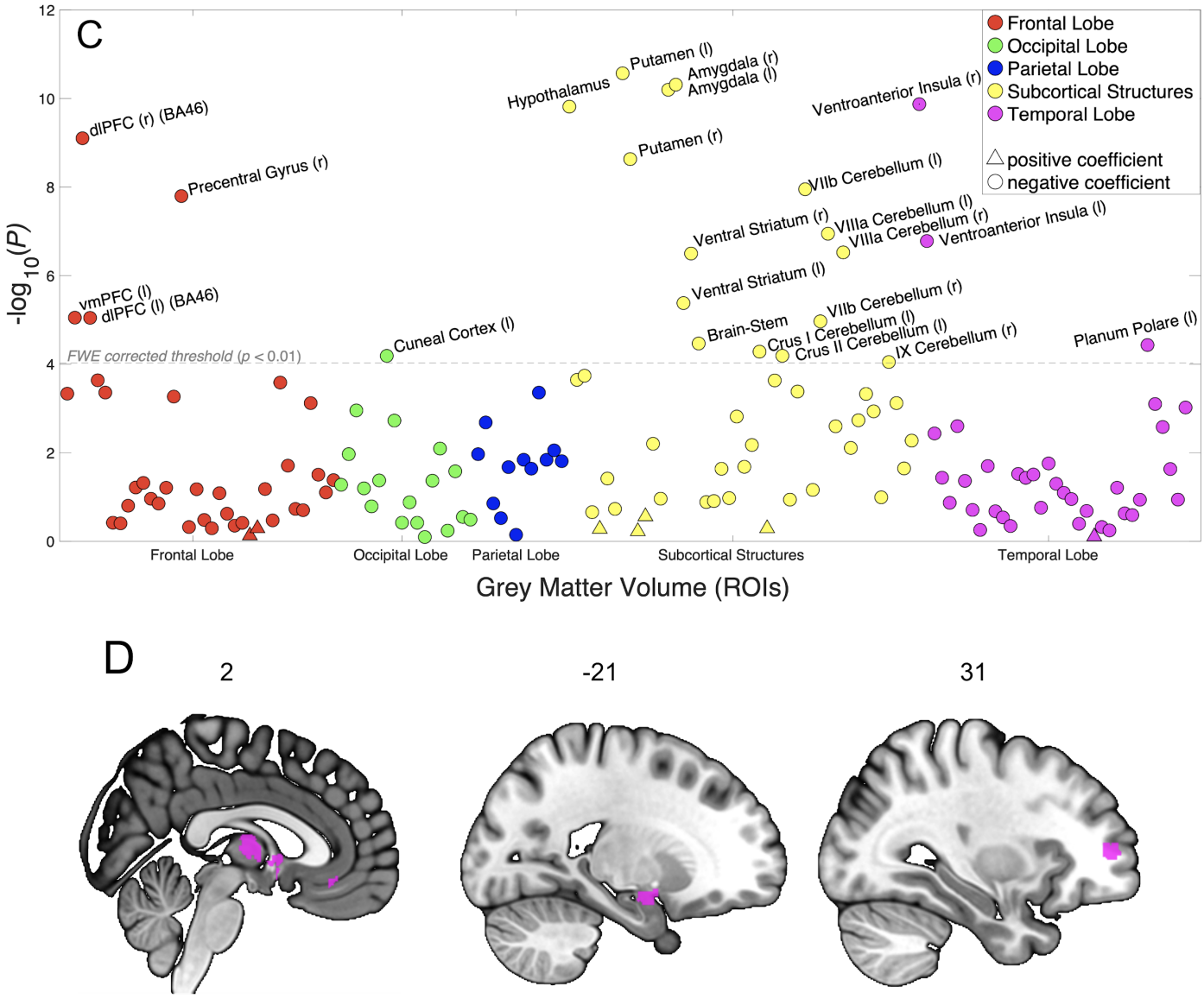

Fig 1. | Association between Risky Behavior and Imaging-Derived Phenotypes (IDPs) of Grey Matter Volume (GMV). (A) Loadings for the first principal component were extracted from four self-reported measures of risky behavior in the *drinking*, *smoking*, *driving* and *sexual* domains (N = 315,855) (see Fig S1 and S2 for descriptive statistics). This first principal component was used as a measure of risky behavior. **(B)** Voxel-level GMV associated with risky behavior (N = 12,675). We observed negative associations in subcortical areas, including *thalamus*, *posterior hippocampus*, *amygdala*, *putamen, ventral striatum* and *cerebellum*. Associations with cortical areas included *posterior middle temporal gyrus*, *precentral gyrus*, *dlPFC*,

anterior insula and *vmPFC*. **(C)** Associations between risky behavior and GMV in 148 regions of interest (ROIs). The grey dotted line shows the family-wise-error corrected threshold of $P = 0.01$ (see SOM for details). **(D)** The conjunction of GMV differences associated with risky behavior reported here and a meta-analysis of 101 fMRI studies based on the key word "risky" revealed overlapping voxels in the thalamus, amygdala, vmPFC and dlPFC (see SOM for details).

Association of Polygenic Risk Scores for Risky Behavior with Grey Matter Volume

Finally, we explored whether participants' genetic disposition for risky behavior, proxied via their polygenic risk scores (PRS), were associated with the neuroanatomical correlates of the trait and whether these associated neuroanatomical correlates mediated the relationship between genetic predisposition and behavior. To this end, we first conducted a GWAS in an independent sample of UKB participants of European ancestry (N=297,025), which excluded all participants with MRI data and their relatives. From the GWAS, we constructed a PRS that aggregated the effects of 1,176,729 single nucleotide polymorphisms (SNPs) of risky behavior for all of the participants with MRI data in our independent target sample (see SOM). The PRS predicted ~3% of the variance in risky behavior in our target sample. Although the PRS was not associated with whole-brain GMV (standardized β = -.004; 95% CI [-.050 .020; $P > 0.41$), it was inversely associated with GMV of distinct areas, specifically the right dlPFC, right putamen and hypothalamus (Fig 2A; regressions included all standard control variables, incl. total intracranial volume). This indicates that GMV in these specific brain areas is associated with the genetic disposition for risky behavior.

Based on these results, we used the previously extracted GMV of these ROIs to examine whether it mediated the observed gene-behavior associations. A structural equation model including all standard controls revealed that ~2.2% of the association between the PRS and risky behavior was mediated through individual differences in GMV in these three regions (indirect path c'; standardized β = 0.004, 95% CI [.002, .005], $P = 1.4 \times 10^{-06}$) (Fig 2B).

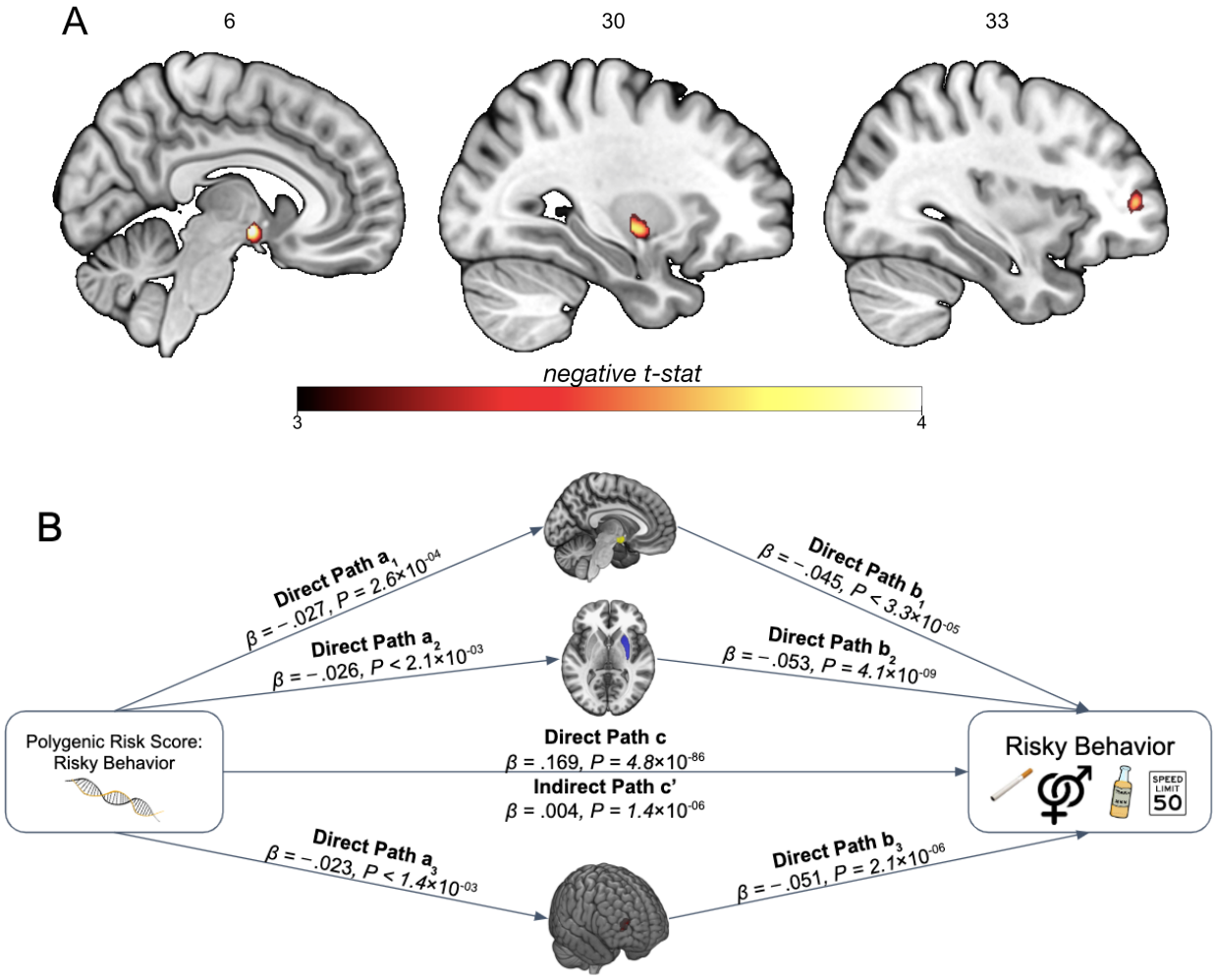

Fig 2. | Association of Polygenic Risk Scores (PRS) for Risk Behavior and Grey Matter Volume (GMV). (A) We constructed a PRS of risky behavior from a GWAS in an independent sample (*N*=297,025) and investigated its associations with GMV in brain voxels that we identified as linked to risky behavior. The PRS was negatively

correlated with GMV in the right dlPFC, putamen and hypothalamus. **(B)** GMV differences in hypothalamus (path 1, designated as a_1 and b_1), right putamen (path 2, designated as a_2 and b_2) and right dlPFC (path 3, designated as a_3 and b_3) mediated ~2.2% of the association between the PRS and risky behavior. Arrows depict the direction of the structural equation modelling and do not imply causality.

Discussion

Taken together, we investigated in a genetically-informed neuroimaging study (a) the association between GMV and real-world risky behavior in a large population sample of European ancestries (*N*=12,675), and (b) how the genetic predisposition for risky behavior is linked to reduced GMV in a network of distinct brain areas.

Several of the areas whose GMVs were linked to risky behavior in this study have also been found to be functionally engaged during risky decision-making in small-scale fMRI studies using stylized tasks. For instance, such correlations have been observed in the aINS, thalamus, dlPFC, vmPFC and VS (*19*, *20*). These findings have led to proposals that upward and downward risks are encoded by distinct circuits, with upward risk mainly represented by areas encoding rewards (VS and vmPFC), and downward risk encoded by areas related to avoidance and negative arousal (aINS). Here, we substantiate these previous functional studies with large-scale evidence that the structural properties of the same areas relate to risky behavior in an ecologically valid setting (*21*), when long-term health or financial consequences are at stake.

Our results extend previous findings by showing that the neural foundation of risky behavior is complex. Our analyses identified additional negative associations between risky behavior and GMV in several areas, including the cerebellum, posterior

hippocampus, hypothalamus, and putamen. While it is not yet entirely clear how structural differences are manifested in functional processes (*22*), our results point to the involvement of manifold neural processes linked to more than the representation and integration of upward and downward risks in the brain. Specifically, considering previous meta-analyses, the areas identified in this study are involved broadly in memory (posterior hippocampus), emotion processing (amygdala, ventro-aINS) (*23*), neuroendocrine processes (hypothalamus) (*24*, *25*), subjective valuation (vmPFC, VS and putamen) (*26*) and executive functions (dlPFC) (*27*). Thus, it appears that risky behavior taps into multiple elements of human cognition, ranging from inhibitory control (*28*) to emotion regulation (*29*) and the integration of outcomes and risks (*30*). This mirrors previous findings showing that risky behavior is also a genetically highly complex trait (*7*).

Additionally, our results underscore the long-suspected role of the hypothalamic–pituitary–adrenal (HPA) axis in regulating risk-related behaviors, in line with hormonal studies that link risky behavior and sensation seeking to stress responsivity (*24*, *25*, *31*). Finally, our finding that risky behavior is linked to the structure of several cerebellar areas confirms the under-appreciated importance of the cerebellum for human cognition and decision-making, and highlights the need for further research on the specific behavioral contributions of this area (*32*). Although more research is needed to examine how structural differences are manifested in functional processes, our results provide evidence that neuro-anatomical structure constitutes the microfoundation for neuro-computational mechanisms underlying individual differences in risky behaviors (*22*).

Several of the observed neuroanatomical correlates of risky behavior were also associated with the genetic disposition for the phenotype. Specifically, we find that GMV

in the hypothalamus, the putamen and the dlPFC share variance with both the genetic factors associated with risky behavior and actual behavior. This finding extends previous correlational (*24*, *30*, *31*) and causal evidence (*25*, *33*) of the involvement of these areas in risky behavior by indicating that a genetic component partly underlies these associations. Although our analyses cannot identify the direction of the causal relationships (see SOM for additional discussion of limitations), they show that risky behavior and its genetic associations share variance with distinct GMV features and provide an overarching framework for how the genetic predispositions for risky behavior may be expressed in the corresponding behavioral phenotype.

Our results are also in line with the bioinformatic annotation of the largest GWAS on risk tolerance to date in over 1 million individuals (*7*), which pointed to specific brain areas in the prefrontal cortex (BA9, BA24), striatum, cerebellum and the amygdala. However, bioinformatics tools used for GWAS annotation cannot be considered conclusive, as they rely on gene expression patterns in relatively small samples of (post-mortem) human brains or non-human samples (*34*), Moreover, they cannot speak to whether changes in a particular tissue or cell type have negative or positive effects on the phenotype or how strong these effects are. Here, we show an alternative approach to annotating GWAS findings using a different type of data (large-scale population samples that include *in-vivo* brain scans and genetic data) and relying on different assumptions than those used by bioinformatics tools. Our results add new insights by showing that lower GMV in specific brain areas is related to more risky behavior and by implicating new brain regions (i.e., putamen, hypothalamus, and dlPFC) in addition to those previously annotated. The effect sizes we identified here (standardized $\beta < 0.08$)

are an order of magnitude larger than those found in GWAS on risky behavior, but they still require very large samples for identification.

Finally, while many features of the brain are heritable, the environment indisputably plays an important role in brain development. We therefore see our results not as independent from, or of greater importance than, the effects of environmental and developmental factors. Rather, our study constitutes one step towards understanding how the complex development of human risk-taking behavior may be constrained by genetic factors.

Acknowledgments:

G.A., R.D, J.K., P.K. and G.N. designed the research plan. G.N., P.K and C.C.R. oversaw the study. G.A. and R.K.L analyzed the data with critical input from P.K., R.D., G.N. and C.C.R. G.A., G.N. and P.K. wrote the paper and Supplementary Materials. All authors contributed to and critically reviewed the manuscript. The authors thank Nadja C. Furtner for helpful comments and Dylan Manfredi for research assistance. The research was conducted using UK Biobank resources under application 40830. The study was supported by funding from an ERC Consolidator Grant to Philipp Koellinger (647648 EdGe), The Wharton School Dean's Research fund to Gideon Nave, and a Swiss National Science Foundation grant to Christian Ruff (100019L_173248). Reagan Wetherill was financially supported by NIAAA K23 grant (K23 AA023894). The work was carried out on the Dutch national e-infrastructure with the support of the SURF Cooperative. Data can be accessed via the UKBiobank, and data analysis scripts are available on OSF (https://osf.io/qkp4g/).

Supplementary Online Materials:

Materials and Methods

Figures S1-S7

Tables S1-S3

References and Notes:

1. F. H. Knight, *Risk, Uncertainty and Profit* (Houghton-Mifflin, New York, 1921).
2. C. C. Eckel, S. C. Füllbrunn, Thar SHE Blows? Gender, Competition, and Bubbles in Experimental Asset Markets. *American Economic Review*. **105** (2015), pp. 906–920.
3. Centers for Disease Control and Prevention, "Incidence, Prevalence, and Cost of Sexually Transmitted Infections in the United States" (CDC , 2013), (available at https://www.cdc.gov/std/stats/sti-estimates-fact-sheet-feb-2013.pdf).
4. J. J. Sacks, K. R. Gonzales, E. E. Bouchery, L. E. Tomedi, R. D. Brewer, 2010 National and

State Costs of Excessive Alcohol Consumption. *Am. J. Prev. Med.* **49**, e73–e79 (2015).

5. L. Blincoe, T. R. Miller, E. Zaloshnja, B. A. Lawrence, "The economic and societal impact of motor vehicle crashes, 2010 (Revised)" (2015), (available at https://trid.trb.org/view/1311862).

6. U.S. Department of Health and Human Services, The Health Consequences of Smoking: 50 Years of Progress. A Report of the Surgeon General. *Atlanta, GA: U.S. Department of Health and Human Services, Centers for Disease Control and Prevention, National Center for Chronic Disease Prevention and Health Promotion, Office on Smoking and Health* (2014).

7. R. Karlsson Linnér, P. Biroli, E. Kong, S. F. W. Meddens, R. Wedow, M. A. Fontana, M. Lebreton, S. P. Tino, A. Abdellaoui, A. R. Hammerschlag, M. G. Nivard, A. Okbay, C. A. Rietveld, P. N. Timshel, M. Trzaskowski, R. de Vlaming, C. L. Zünd, Y. Bao, L. Buzdugan, A. H. Caplin, C.-Y. Chen, P. Eibich, P. Fontanillas, J. R. Gonzalez, P. K. Joshi, V. Karhunen, A. Kleinman, R. Z. Levin, C. M. Lill, G. A. Meddens, G. Muntané, S. Sanchez-Roige, F. J. van Rooij, E. Taskesen, Y. Wu, F. Zhang, 23and Me Research Team, eQTLgen Consortium, International Cannabis Consortium, Social Science Genetic Association Consortium, A. Auton, J. D. Boardman, D. W. Clark, A. Conlin, C. C. Dolan, U. Fischbacher, P. J. F. Groenen, K. M. Harris, G. Hasler, A. Hofman, M. A. Ikram, S. Jain, R. Karlsson, R. C. Kessler, M. Kooyman, J. MacKillop, M. Männikkö, C. Morcillo-Suarez, M. B. McQueen, K. M. Schmidt, M. C. Smart, M. Sutter, A. R. Thurik, A. G. Uitterlinden, J. White, H. de Wit, J. Yang, L. Bertram, D. I. Boomsma, T. Esko, E. Fehr, D. A. Hinds, M. Johannesson, M. Kumari, D. Laibson, P. K. E. Magnusson, M. N. Meyer, A. Navarro, A. A. Palmer, T. H. Pers, D. Posthuma, D. Schunk, M. B. Stein, R. Svento, H. Tiemeier, P. R. H. J. Timmers, P. Turley, R. J. Ursano, G. G. Wagner, J. F. Wilson, J. Gratten, J. J. Lee, D. Cesarini, D. J. Benjamin, P. D. Koellinger, J. P. Beauchamp, Genome-wide association analyses of risk tolerance and risky behaviors in over 1 million individuals identify hundreds of loci and shared genetic influences. *Nat. Genet.* **51**, 245–257 (2019).

8. L. T. Elliott, K. Sharp, F. Alfaro-Almagro, S. Shi, K. L. Miller, G. Douaud, J. Marchini, S. M. Smith, Genome-wide association studies of brain imaging phenotypes in UK Biobank. *Nature*. **562**, 210–216 (2018).

9. P. M. Thompson, T. D. Cannon, K. L. Narr, T. van Erp, V. P. Poutanen, M. Huttunen, J. Lönnqvist, C. G. Standertskjöld-Nordenstam, J. Kaprio, M. Khaledy, R. Dail, C. I. Zoumalan, A. W. Toga, Genetic influences on brain structure. *Nat. Neurosci.* **4**, 1253–1258 (2001).

10. M. A. Grubb, A. Tymula, S. Gilaie-Dotan, P. W. Glimcher, I. Levy, Neuroanatomy accounts for age-related changes in risk preferences. *Nat. Commun.* **7**, 13822 (2016).

11. W. H. Jung, S. Lee, C. Lerman, J. W. Kable, Amygdala Functional and Structural Connectivity Predicts Individual Risk Tolerance. *Neuron*. **98**, 394–404.e4 (2018).

12. Z. Nasiriavanaki, M. ArianNik, A. Abbassian, E. Mahmoudi, N. Roufigari, S. Shahzadi, M. Nasiriavanaki, B. Bahrami, Prediction of individual differences in risky behavior in young adults via variations in local brain structure. *Front. Neurosci.* **9**, 359 (2015).

13. K. S. Button, J. P. A. Ioannidis, C. Mokrysz, B. A. Nosek, J. Flint, E. S. J. Robinson, M. R. Munafò, Power failure: why small sample size undermines the reliability of neuroscience. *Nat. Rev. Neurosci.* **14**, 365–376 (2013).

14. T. Dohmen, A. Falk, D. Huffman, U. Sunde, J. Schupp, G. G. Wagner, INDIVIDUAL RISK ATTITUDES: MEASUREMENT, DETERMINANTS, AND BEHAVIORAL CONSEQUENCES. *Journal of the European Economic Association*. **9** (2011), pp. 522–550.

15. L. R. Cardon, L. J. Palmer, Population stratification and spurious allelic association. *Lancet*. **361**, 598–604 (2003).

16. D. Romer, Adolescent risk taking, impulsivity, and brain development: implications for prevention. *Dev. Psychobiol.* **52**, 263–276 (2010).

17. H. R. Kranzler, R. Wetherill, R. Feinn, T. Pond, J. Gelernter, J. Covault, Posttreatment effects of topiramate treatment for heavy drinking. *Alcohol. Clin. Exp. Res.* **38**, 3017–3023 (2014).

18. T. Yarkoni, R. A. Poldrack, T. E. Nichols, D. C. Van Essen, T. D. Wager, Large-scale automated synthesis of human functional neuroimaging data. *Nat. Methods*. **8**, 665–670 (2011).

19. P. N. C. Mohr, G. Biele, H. R. Heekeren, Neural processing of risk. *J. Neurosci.* **30**, 6613–6619 (2010).

20. C. C. Wu, M. D. Sacchet, B. Knutson, Toward an affective neuroscience account of financial risk taking. *Front. Neurosci.* **6**, 159 (2012).

21. T. Schonberg, C. R. Fox, R. A. Poldrack, Mind the gap: bridging economic and naturalistic risk-taking with cognitive neuroscience. *Trends Cogn. Sci.* **15**, 11–19 (2011).

22. J. W. Kable, I. Levy, Neural markers of individual differences in decision-making. *Curr Opin Behav Sci*. **5**, 100–107 (2015).

23. L. J. Chang, T. Yarkoni, M. W. Khaw, A. G. Sanfey, Decoding the role of the insula in human cognition: functional parcellation and large-scale reverse inference. *Cereb. Cortex*. **23**, 739–749 (2013).

24. B. E. Evans, K. Greaves-Lord, A. S. Euser, I. H. A. Franken, A. C. Huizink, The relation between hypothalamic-pituitary-adrenal (HPA) axis activity and age of onset of alcohol use. *Addiction*. **107** (2012), pp. 312–322.

25. M. J. Kreek, D. A. Nielsen, E. R. Butelman, K. S. LaForge, Genetic influences on impulsivity, risk taking, stress responsivity and vulnerability to drug abuse and addiction. *Nat. Neurosci.* **8**, 1450–1457 (2005).

26. J. O'Doherty, P. Dayan, J. Schultz, R. Deichmann, K. Friston, R. J. Dolan, Dissociable roles of ventral and dorsal striatum in instrumental conditioning. *Science*. **304**, 452–454 (2004).

27. N. U. F. Dosenbach, D. A. Fair, A. L. Cohen, B. L. Schlaggar, S. E. Petersen, A dual-networks architecture of top-down control. *Trends Cogn. Sci.* **12**, 99–105 (2008).

28. I. Ivanov, K. P. Schulz, E. D. London, J. H. Newcorn, Inhibitory control deficits in childhood and risk for substance use disorders: a review. *Am. J. Drug Alcohol Abuse*. **34**, 239–258 (2008).

29. R. M. Heilman, L. G. Crişan, D. Houser, M. Miclea, A. C. Miu, Emotion regulation and decision making under risk and uncertainty. *Emotion*. **10**, 257–265 (2010).

30. P. N. Tobler, G. I. Christopoulos, J. P. O'Doherty, R. J. Dolan, W. Schultz, Risk-dependent reward value signal in human prefrontal cortex. *Proc. Natl. Acad. Sci. U. S. A.* **106**, 7185–7190 (2009).

31. A. C. Huizink, R. F. Ferdinand, J. Ormel, F. C. Verhulst, Hypothalamic-pituitary-adrenal axis activity and early onset of cannabis use. *Addiction*. **101**, 1581–1588 (2006).

32. R. L. Buckner, The cerebellum and cognitive function: 25 years of insight from anatomy and neuroimaging. *Neuron*. **80**, 807–815 (2013).

33. D. Knoch, L. R. R. Gianotti, A. Pascual-Leone, V. Treyer, M. Regard, M. Hohmann, P. Brugger, Disruption of right prefrontal cortex by low-frequency repetitive transcranial magnetic stimulation induces risk-taking behavior. *J. Neurosci.* **26**, 6469–6472 (2006).

34. Allen Institute for Brain Science, BrainSpan atlas of the developing human brain (2015), (available at http://www.brainspan.org/).

Supplementary Materials for

Genetic Underpinnings of Risky Behavior Relate to Altered Neuroanatomy

Materials and Methods

1. Sample Characteristics and Selection Criteria

We used publicly available data from the UK Biobank (UKB), which recruited 502,617 people aged 40 to 69 years from the general population across the United Kingdom (*1*, *2*). All UKB participants provided written informed consent and the study was granted ethical approval by the North West Multi-Centre Ethics committee. UKB participants completed extensive batteries of tests, questionnaires and lifestyle measures, which have enabled researchers to investigate genetic, neural and behavioral associations that are detectable only in large samples [e.g., (*3*)].

Our initial sample consisted of N = 18,796 individuals with brain scans and genotype data, all of the imaged UKB participants as of 18 Oct 2018. We excluded 923 subjects with problematic genotype data (N = 14), putative sex chromosome aneuploidy (N = 6), a mismatch between genetic and reported sex (N = 10) or non-European ancestry (N = 893).

To minimize the potential influence of neurotoxic effects due to excessive alcohol intake (*4*), we excluded past or current heavy drinkers from the sample (531 female and 793 male participants), where heavy drinking was defined as consuming more than 24 drinks per week for males and more than 18 drinks per week for females (*5*). To exclude potential former drinkers, we also removed 426 participants who indicated that they don't drink alcohol.

All of the structural T1 MRI images used in the study underwent automated quality control by the UKB brain imaging processing pipeline (*6*). We ran additional quality checks on the images

using the Computational Anatomy Toolbox (CAT; www.neuro.uni-jena.de/cat/) for SPM (www.fil.ion.ucl.ac.uk/spm/software/spm12/). This resulted in the removal of additional 747 individuals who exhibited substantial image inhomogeneity (overall volume correlation below two standard deviations from the mean). Finally, we removed all participants with incomplete behavioral data of interest or control variables (N = 2,701). Our final dataset consisted of N = 12,675 individuals.

2. Measures

2. 1. Risky behavior measure

We closely followed the methods of (*7*) and derived a measure of risky behavior based on participants' self-reports across the drinking, smoking, driving, and sexual domains.

Specifically, we used the following UK Biobank variables:

- Lifetime number of sexual partners (Data-Field 2149)[1]
- Number of alcoholic drinks per week (Data-Fields: 1558, 1568, 1578, 1588, 1598, 1608, 5364, 4407, 4418, 4429, 4440, 4451, 4462)
- Ever smoking (Data-Field 20116, 1249, 1239)
- Frequency of driving faster than the motorway speed limit (Data-Field 1100)

The exact description of each Data-Field can be found in the online data showcase of the UKB (http://biobank.ctsu.ox.ac.uk/crystal/search.cgi). The annotated STATA code that we used to derive the behavioral phenotypes and control variables for our analyses can be found in our pre-registered analysis plan (https://osf.io/qkp4g/).

All variables above were measured on at least one of 3 occasions: (1) the initial assessment visit, (2) the first repeat assessment visit, and (3) the imaging visit. Data from (2) and (3) are only

[1] Self-reports of the number of sexual partners have been implicated in risky behaviors related to alcohol abuse (i.e., binge drinking) and unprotected sex, specifically in young adults (*8*), irrespective of gender or sexual orientation.

available for a subset of the original sample. In the case where participants provided answers across more than one visit, we computed the average of their reports.

To obtain a measure that captures the common variance in risky behavior shared across the driving, drinking, smoking, and sexual domains, we performed principal component analysis (PCA) on *N* = 315,855 UKB subjects and extracted the first principal component as our main outcome of interest for this study (referred to as "risky behavior").

Compared to experimental procedures that elicit risk tolerance, self-reported measures exhibit higher external validity and test-retest reliability (*9–11*). Furthermore, by extracting the first principal component of the four risky behaviors, we reduce measurement noise due to the aggregation of signal across various measures, while capturing behavioral tendencies across domains that are independent of idiosyncratic differences in the four specific behaviors.

2.2 Control Variables

Our analyses on the relationships between brain anatomy and risky behavior systematically controlled for several genetic, socio-demographic and anthropometric factors, which could potentially confound the observed associations [e.g. sex (*12*), height (*13*) and genetic population structure (*14*)]. Specifically, all of our analyses used the following control variables, which were provided by the UKB:

- Age at the time of brain scan (Data-Field 21003)
- Birth year dummies (Data-Field 33)
- Sex (self reported and genetically identified, Data-Fields 31 & 22001)
- Height (Data-Field 50)
- Handedness (Data-Field 1707, categorical variable: Right-handed, Left-handed, ambidextrous, NA)
- Sex x birth year interactions (binned into fields containing at least 20 subjects each)
- The first 40 PCs of the genetic data (Data-Field 22009)
- Total intracranial volume (TIV), derived using the CAT12 toolbox.

The empirical distributions of the main variables used in our analysis and the correlations between them are depicted in Fig S1 and Fig S2**.**

2.3 Imaging-derived Phenotypes (IDPs)

2.3.1 T1 MRI Image Processing

Our voxel-level analysis used T1-weighted structural brain MRI images in NIFTI format provided by the UKB (data field 20252). The images were acquired using a 3-T Siemens Skyra scanner, with a 32-channel head coil (Siemens, Erlangen, Germany), with the following scanning parameters: repetition time = 2000 ms; echo time = 2.1 ms; flip angle = 8°; matrix size = 256 × 256 mm; voxel size = 1 × 1 × 1 mm; number of slices = 208.

We preprocessed the data using the Computational Anatomy Toolbox (CAT; www.neuro.uni-jena.de/cat/) for SPM (www.fil.ion.ucl.ac.uk/spm/software/spm12/), a fully automated toolbox for deriving neuroanatomical measurements at voxel and ROI levels. Image pre-processing used the default setting of CAT12 (accessible online at http://www.neuro.uni-jena.de/cat12/CAT12-Manual.pdf). Images were corrected for bias-field inhomogeneities, segmented into gray matter, white matter, and cerebrospinal fluid (CSF), spatially normalized to the MNI space using linear and non-linear transformations, and were modulated to preserve the total amount of signal in the original image during spatial normalization (the specific SPM-processing parameters can be found in the pre-registered document on OSF https://osf.io/qkp4g/). We applied spatial smoothing with 8-mm Full-Width-at-Half-Maximum (FWHM) Gaussian kernel for the segmented, modulated images for grey matter volume (GMV). Finally, to ensure that only voxels that likely contained grey matter entered the analyses, we constructed a brain mask based on the average of all GMV images. Specifically, following standard VBM procedures (see SPM/CAT12 http://www.neuro.uni-jena.de/cat12/CAT12-Manual.pdf) we thresholded the average of all brain images at 250 (GMV intensity units). The resulting image was binarized and applied as a pre-mask to all individual images before running analyses. Additionally, on an individual level, we

excluded all voxels from the analyses that exhibited a lower grey matter volume than .1 (see standard parameters of SPM/CAT12 http://www.neuro.uni-jena.de/cat12/CAT12-Manual.pdf).

2.3.2 Region of interest (ROI)-level IDPs Processed by the UKB

We used all of the GMV IDPs that were processed and provided by the UKB [for details see (*6*)]. These phenotypes include GMV of 139 ROIs derived from parcellations from the Harvard-Oxford cortical and subcortical atlases, and Diedrichsen cerebellar atlas.

2.3.3 Additional ROI-level IDPs

Based on our voxel-level results (see 3.1), we extracted 5 additional ROI-level IDPs that quantified GMV in anatomical substructures that were not derived by the UKB. These ROIs were extracted bilaterally from unbiased masks and included the dorsolateral prefrontal cortex (dlPFC; BA 46), hypothalamus, posterior hippocampus, ventro-anterior insula and ventromedial prefrontal cortex (vmPFC). For the dlPFC, ventro-anterior insula and vmPFC masks, we used recent functional parcellations based on resting state data. The dlPFC mask was derived using the Sallet Dorsal Frontal resting state connectivity-based parcellation (cluster 7/BA46) (*15*). Functionally, this area exhibits coupling with the frontal-parietal network (incl. anterior cingulate cortex, parietal cortex and inferior parietal lobe), as well as with the vmPFC. Anatomically, its boundaries show resemblance to BA 46 - an area functionally related to executive function that shows distinct cytoarchitectonic properties.

We extracted GMV from the vmPFC using a parcellation of the medial wall of the prefrontal cortex, based on resting state functional coupling (*16*). Specifically, we extracted GMV from 14m - an area linked to cost-benefit integration in value-based decision-making (*17–20*), which maintains strong positive coupling with hypothalamus, ventral striatum, and amygdala (*21*). The hypothalamus mask was derived from a high-resolution atlas of human subcortical brain nuclei (*22*). The posterior hippocampus mask was derived according to recent recommendations for

long-axis segmentation of the hippocampus in human neuroimaging (*23*). We labeled hippocampal voxels posterior to the coronal plane at y = -21 in MNI space (which corresponds to the uncal apex of the parahippocampal gyrus), as posterior hippocampus. To ensure spatial precision across participants, we used a minimum 80% likelihood of each voxel being in the anatomical structure for all of the aforementioned masks. The ventro-anterior insula mask was derived following a recent parcellation of the insula based on a resting state functional connectivity analysis by (*24*), who reported that this brain region showed functional coactivation with limbic areas including amygdala, ventral tegmental area (VTA), superior temporal sulcus, and posterolateral orbitofrontal cortex. The raw mask was thresholded at z = 10.

2.4 Polygenic Risk Score (PRS) for Risky Behavior

We used the genetic data provided by the UKB to construct a polygenic risk score (PRS) for risky behavior. As a first step, we reran the genome-wide association study (GWAS) of risky behavior (the same measure used in the current study) as reported in (*7*)[2] after excluding the 18,796 genotyped individuals with usable T1 NIFTI structural brain images (UKB field 20252) and all of their relatives up to the third degree. Relatives were defined using the KING coefficient (*25*) based on a pairwise coefficient >0.0442. The final GWAS sample included 297,025 individuals of European ancestry. We used BOLT-LMM version 2.3.2 (*26*) to perform GWAS with linear mixed models (LMM), which outperforms linear regression in terms of statistical power and controlling for relatedness (*27*).

Next, we performed quality control (QC) of the GWAS results using a standardized QC protocol, described in detail in (*7*). This protocol removes rare and low-quality single-nucleotide polymorphisms (SNPs) based on minor allele frequency (MAF) < 0.001, imputation quality (INFO)

[2] In Karlsson Linnér et al. (2019), the phenotype 'risky behavior' as defined here was referred to as the 'first PC of the four risky behaviors'.

< 0.7, and SNPs that could not be aligned with the Haplotype Reference Consortium (HRC) reference panel. After QC, a total of 11,514,220 SNPs remained in the GWAS summary statistics. We estimated genetic correlations between our GWAS on risky behavior (N = 297,025) and 85 other traits with bivariate LD Score regression (*28*). The estimates are reported in Table S1. For this purpose, we queried the "GWAS ATLAS" (*29*) to identify publicly archived GWAS results that we considered relevant. We supplemented the publicly available GWAS with a soon-to-be published GWAS on diet composition (*30*). Notably, the collected traits span across many different outcomes, including the anthropometric, behavioral, cognitive, psychiatric, medical, and socioeconomic domains.

We found moderate to strong genetic correlations with a range of phenotypes that are considered risky behaviors, including ever consuming cannabis (r_g = 0.72; SE = 0.03), self-employment (r_g = 0.52; SE = 0.30), and age at first sexual experience (r_g = –0.54; SE = 0.02). Our measure of risky behavior was also genetically correlated with a range of mental disorders including bipolar disorder (r_g = 0.23; SE = 0.03), major depressive disorder (r_g = 0.22; SE = 0.03), and schizophrenia (r_g = 0.17; SE = 0.02). Lastly, risky behavior is genetically correlated in the expected direction with the personality phenotypes such as conscientiousness (r_g = –0.25; SE = 0.10) and extraversion (r_g = 0.34; SE = 0.05).

Thereafter, we calculated for each participant *i* a PRS, S_i, by weighting her or his genotype across *j* SNPs, g_{ij}, with the regression coefficients, β_j, that we estimated in the GWAS described above. Thus, the PRS was a linear combination of genetic effects, calculated as:

$$S_i = \sum_{j=1}^{M} \beta_j g_{ij},$$

where the set of SNPs, M, was restricted to the consensus genotype set of 1.4 million SNPs established by the International HapMap 3 Consortium (*31*), which has been successfully employed for polygenic prediction in many previous studies. In addition, the PRS was constructed only with autosomal, bi-allelic SNPs with MAF > 0.01 and $INFO$ > 0.9 in the UKB.

The resultant PRS was based on a total of *M*=1,176,729 SNPs. The PRS was then standardized to mean zero and unit variance in the prediction sample.

3. Analysis

3.1 Voxel-based Morphometry (VBM) Analyses of Risky Behavior and Associated PRS

We identified associations between risky behavior and localized GMV using whole-brain voxel-based morphometry (VBM), a method that normalizes the anatomical brain images of all participants in one stereotactic space (*32*). We regressed risky behavior separately on each voxel of the smoothed GMV images (see 2.3.1) while controlling for all aforementioned control variables. We corrected for multiple hypothesis testing by adjusting the family-wise-error rate to $\alpha = 0.01$ using permutation tests ($p_{uncorr} = 1.248 \times 10^{-06}$, with $t_{uncorr} = 4.85$, see 3.6 for details; see Fig S3 and Table S2 for the summary statistics of each cluster and the coordinates of the peak voxel within that cluster). As a robustness check, we performed parametric tests using SPM and obtained qualitatively similar results.

3.2 Region of Interest (ROI)-level Analysis

We conducted an additional analysis at the ROI level, which investigated the associations between risky behavior and 139 IDPs of GMV extracted by the UKB brain imaging processing pipeline (*6*)[3] in addition to the 9 IDPs that we derived based on the voxel-level analysis (see *2.3.3*). We regressed risky behavior separately on each IDP while controlling for the standard control variables listed in 2.2 and corrected for multiple hypothesis testing by adjusting the family-wise-error rate of $\alpha = 0.01$ using permutation tests ($p_{uncorr} = 9.37 \times 10^{-05}$, with $t_{uncorr} = 3.91$, see 3.6 for details).

[3] These IDPs were extracted using parcellations from the Harvard-Oxford cortical and subcortical atlases and Diedrichsen cerebellar atlas, and consists of all the GMV IDPs derived by the UKB as for August 2019.

3.3 Comparison of VBM Results with a Meta-Analysis of Functional MRI (fMRI) Studies

To compare our VBM results with activation patterns reported in functional MRI (fMRI) studies of risky behaviors, we utilized the results of an openly available meta-analysis provided by Neurosynth (*33*), an online platform for large-scale, automated synthesis of fMRI data (https://neurosynth.org/). The meta-analysis, which was based on the key word 'risky', consisted of K = 101 individual studies with a total of N = 4,717 participants and was conducted using a uniformity test (assuming that random activations are evenly distributed across all voxels). The meta-analytic statistical image was corrected for multiple comparisons by applying a false discovery rate (FDR) of .01 (implemented by Neurosynth), which corresponds to a false positive rate of 1% for all voxels showing activation. For the summary of studies included in the meta-analysis see Table S3. The 3D activation map that resulted from the meta analysis is available on https://neurosynth.org/analyses/terms/risky/. We compared our VBM results (see 3.1) and the meta-analysis by performing a whole-brain voxel-level conjunction analysis between the two (see Fig. S6). Specifically, the conjunction exhibits the overlap of all voxels that reached significance in the VBM analysis as well as in the meta-analysis.

3.4 Voxel-based Morphometry (VBM) Analyses of Risky Behavior PRS

To identify whether the voxels identified to be associated with risky behavior were also associated with the trait's PRS, we repeated the VBM analysis in these voxels using the PRS as the dependent variable (instead of the phenotypic risky behavior measure). This approach allowed us to identify brain regions that were likely to mediate the effect of genes on risky behavior. As the PRS was constructed using GWAS results from an independent sample, the effect size estimates in this analysis were not inflated due overfitting. We again accounted for multiple comparisons using a permutation test with a family-wise-error rate of $p_{FWE} < 0.05$ (see 3.6). This part of the analysis was not pre-registered and is considered exploratory.

3.5 Mediation Analysis

We identified three brain regions whose GMVs were associated with the PRS of risky behavior (right dlPFC, right putamen and hypothalamus). To test whether GMV differences in these regions mediated the association between PRS and risky behavior, we conducted a mediation analysis in STATA 14. We first extracted GMV from all these ROIs using the same unbiased masks as in the ROI analysis (see 2.3.3). Then, we performed a structural equation modeling (SEM) analysis to estimate the effect of the PRS on risky behavior that was mediated via GMV differences in each of the three ROIs. All SEM equations included the aforementioned standard control variables listed in 2.2. We carried out an additional robustness check by estimating a SEM that assumed one single path (i.e. the sum of all ROIs). This analysis provides qualitatively the same pattern of results (see Fig. S7).

3.6 Family-Wise-Error Correction using Permutation Tests:

To account for multiple hypothesis testing, we determined the appropriate family-wise error corrected *p*-value threshold with a permutation test procedure in each of our analyses (*34*). To this end, we generated 1,000 datasets with randomly permuted phenotypes (i.e., breaking the link between the dependent and explanatory variables), estimated regression models for all IDPs per analysis, and recorded the lowest *p*-value of each run to generate an empirical distribution of the test statistic under the null hypothesis. To obtain the family-wise error rate of any given alpha, we used the *n*th = alpha x 1000 lowest *p*-value from the 1,000 permutation runs as the uncorrected *p*-value threshold.

4. Extended Discussion of Results - Limitations and Possible Confounds

Our study highlights the importance of using large samples to study associations of neuroanatomy with complex behavioral traits. The largest effect we identified for the relationship between any cluster of voxels and risky behavior was $\Delta R^2 = 0.6\%$ (see Table S2). It would require more than 1,750 participants to have 90% statistical power at a liberal *p*-value threshold of 0.05

(uncorrected) to identify effects of this magnitude. This is a lower bound for the required sample size for such studies and does not reflect the fact that our effect size estimate is biased upward by the statistical "winner's curse" and the need to correct for multiple testing. Previous large-scale VBM studies ($N > 1000$) with other behavioral phenotypes (*35*) found effect sizes of similar magnitude and suggest that large samples are a prerequisite to detect such an association reliably. Of note, the largest previous study of risk tolerance employed a sample of 108 participants (*36*) and would have only 12% power to detect $\Delta R^2 = 0.6\%$ at $\alpha = 0.05$ (uncorrected).

While our analyses identify distinct brain areas that mediate gene-phenotype associations for risky behavior (i.e., putamen, hypothalamus and dlPFC), they do not address their causal relationship. For instance, it is possible that a person's genetic disposition would lead them to self-select environments that influence both risky behavior and features of brain anatomy. Furthermore, while our study is larger and more representative than any previous investigation of the topic, and although we controlled for many potential confounds, it was conducted in a population of UK individuals of European descent that were over 40 years old at the time of measurement, which limits the generalizability of our results to other populations. Moreover, our results do not exclude the possibility of other possible unobserved confounds that our analyses did not account for.

Nonetheless, with the rise of large publicly available data sets [e.g. (*37*)], we are confident that future studies will be able to test whether our findings generalize to populations of different ethnicities and age groups (e.g., adolescents), and the extent to which they generalize to other cognitive and behavioral traits (e.g., general cognitive ability (*38*), self-control and other domains of decision-making).

5. Pre-registration of Analysis Plan and Unplanned Deviations

We pre-registered our analysis plan on Open Science Framework (OSF, https://osf.io/qkp4g/). Our pre-registered plan specifies the construction of the dependent variable, the control

variables, the inclusion criteria and quality controls, the VBM analyses and the main ROI-level analyses.

We deviated from the pre-registered plan in several cases, which are documented in the project's page on OSF. These deviations occurred when the computational burden of following the pre-registered plan was unexpectedly high, and when alternative measures that we were not aware of at the time of the pre-registration were made available by the UKB. Specifically, we decided not to use alternative segmentations of the cortex (e.g. Hammer's atlas) as robustness checks for our ROI-level analysis because of the significant computational burden in deriving those measures. Instead, based on the voxel-level analysis, we derived additional ROIs only when they were not derived in sufficient granularity in the IDPs provided by the UKB (see 2.3.3).

Similarly, we did not derive cortical thickness (CT) measures because of the high computational burden using FreeSurfer, which is the gold standard in cortical thickness estimation. While other means to derive CT would have been available (e.g. CAT toolbox), they would provide relatively lower quality data and would not allow analyses of subcortical areas. Additionally, the UKB is expected to release CT measures derived from FreeSurfer in the near future (see the UKB Data Showcase website for public announcements). The lack of CT measures has also led us to decide to postpone the conduct of an additional pre-registered multivariate analysis.

Finally, our pre-registered plan stated that we would run additional robustness checks to control for potential neurotoxic effects of excessive alcohol intake. However, upon examining the data for a different project that is focused on the effects of alcohol intake on the brain, we observed effects that were mainly driven by individuals who were heavy drinkers. We therefore decided to deviate from our original plan and exclude all participants who qualified as current or former regular heavy drinkers (see SOM 1). However, we also provide robustness checks that include weekly alcohol intake as a covariate. Finally, the pre-registered analysis of white-matter volume is not reported here, but will be provided in a subsequent publication.

6. Code Availability

The software and code used in this study are publicly available, including STATA and Matlab scripts (OSF, https://osf.io/qkp4g/).

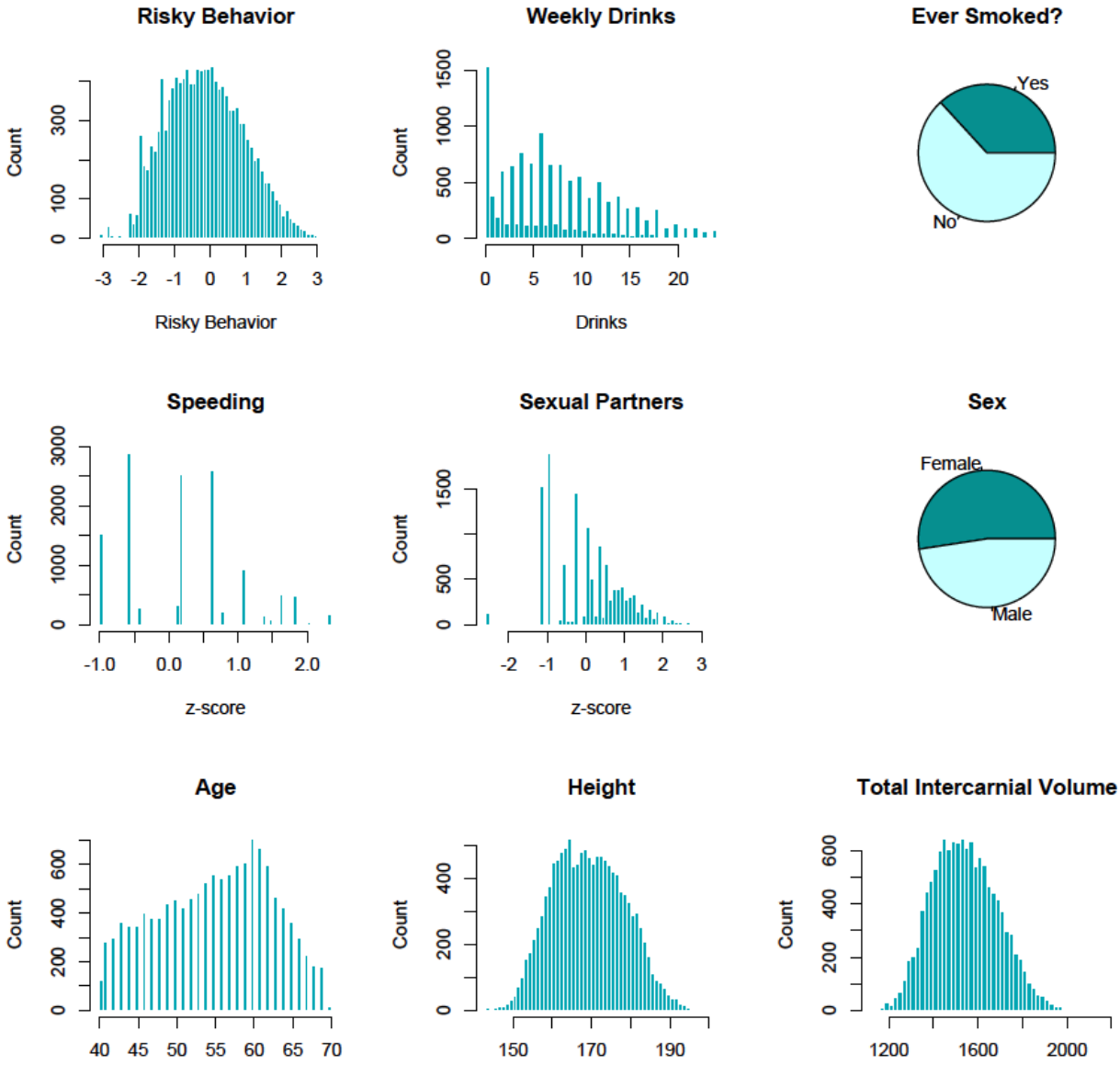

Fig S1. | Empirical distributions of the main variables used in the study.

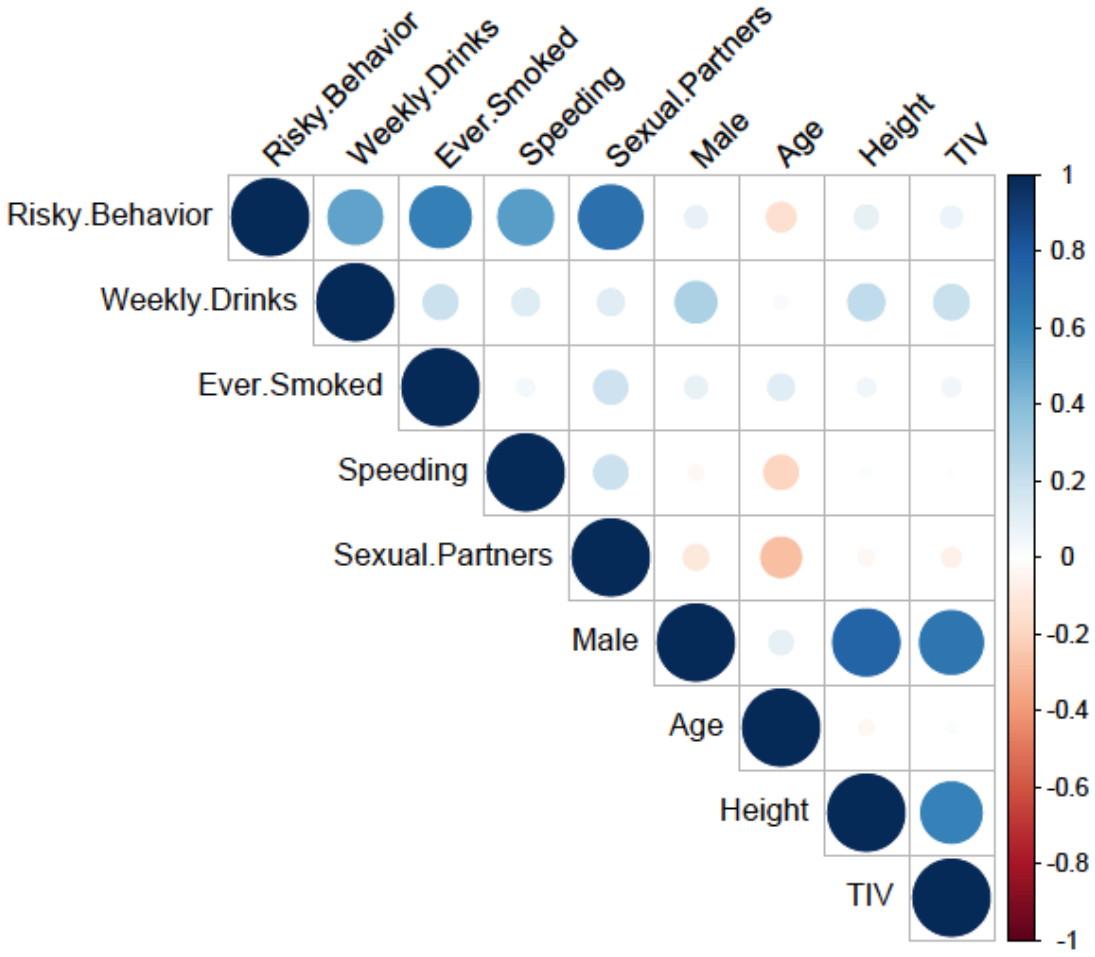

Fig S2. | Bivariate correlations between the main variables used in the study.

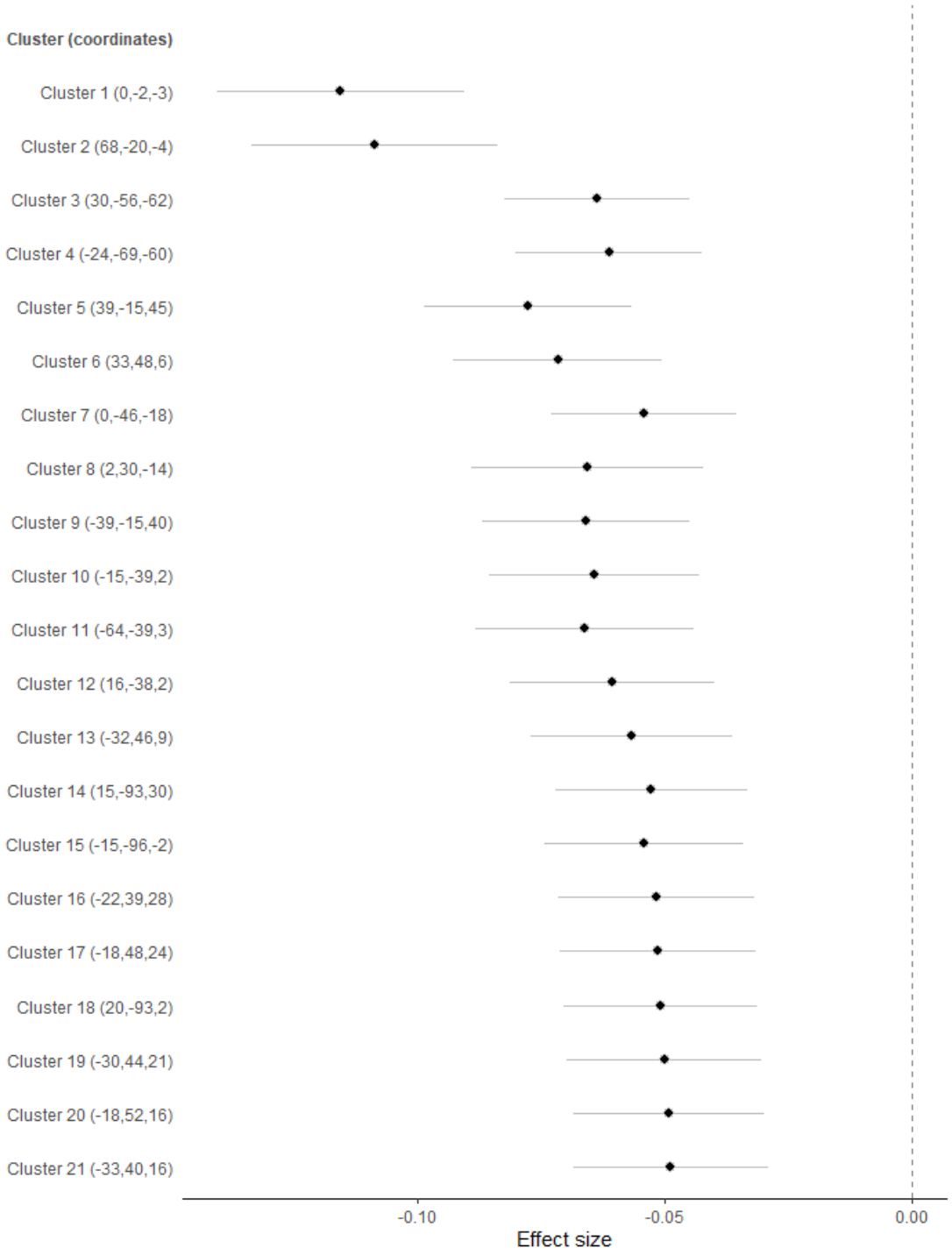

Fig S3. | Association between risky behavior and clusters of voxels of grey matter volume (GMV). Depicted are the effect sizes (i.e. standardized betas) with uncorrected 95% confidence intervals of each cluster showing association with risky behavior at a significance level of *P* = 1% (FWE-corrected) (see Table S2 for more details). Coordinates of peak activation for each cluster are reported in parentheses (in mm).

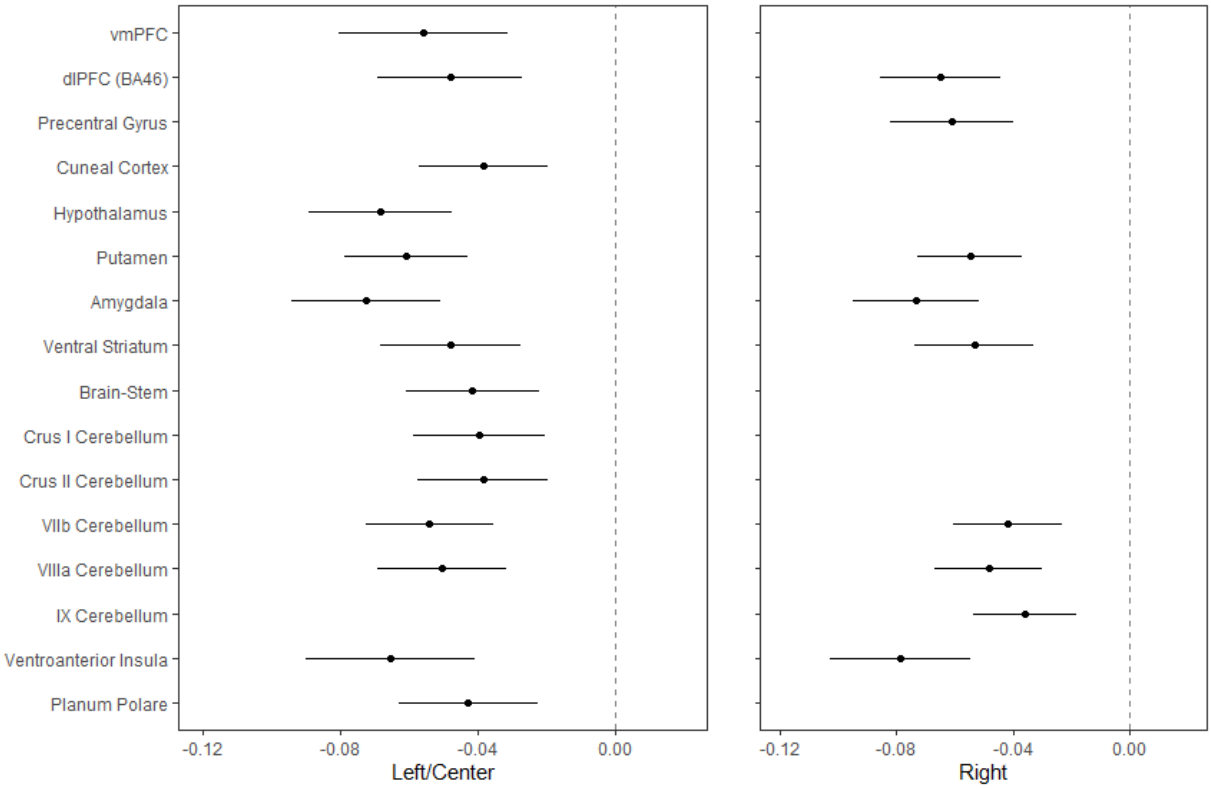

Fig S4. | Association between risky behavior and IDPs of grey matter volume (GMV). Depicted are the effect sizes (i.e. standardized betas) with uncorrected 95% confidence intervals of each ROI showing association with risky behavior at a significance level of *P* = 1% (FWE-corrected).

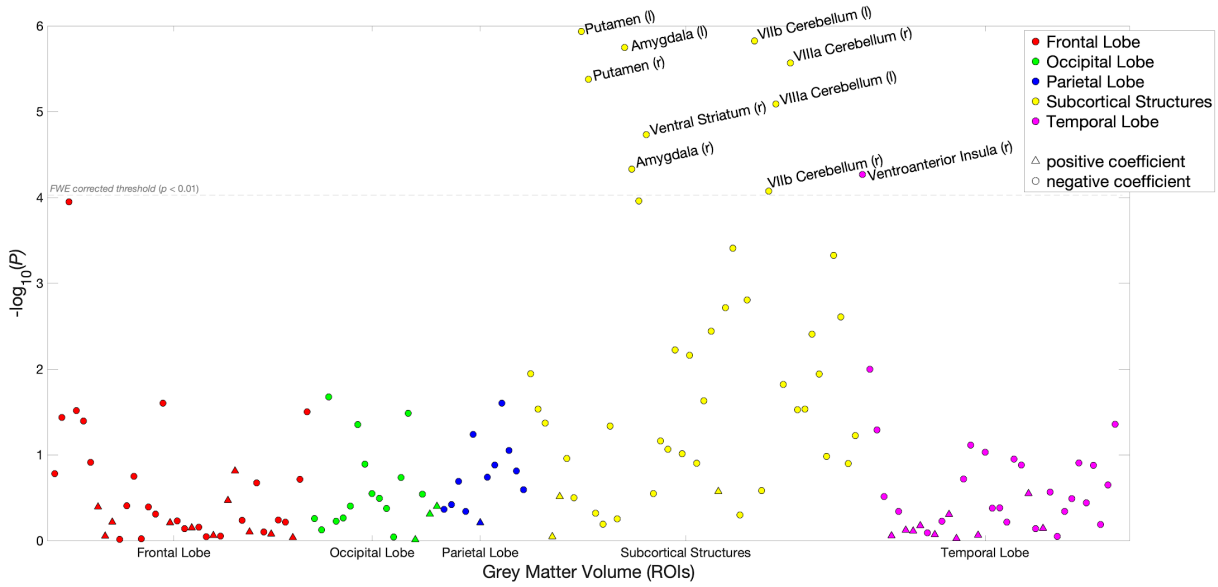

Fig S5. | Robustness check of associations between risky behavior and imaging-derived phenotypes (IDPs) of grey matter volume (GMV). Depicted are the associations between risky behavior and grey matter volumes in 148 ROIs, while controlling for alcohol intake in addition to all of our standard controls (*N* = 12,675). Due to potential neurotoxic effects of heavy drinking, we excluded participants who reported drinking more than 18 (for females) or 24 (for males) drinks per week.

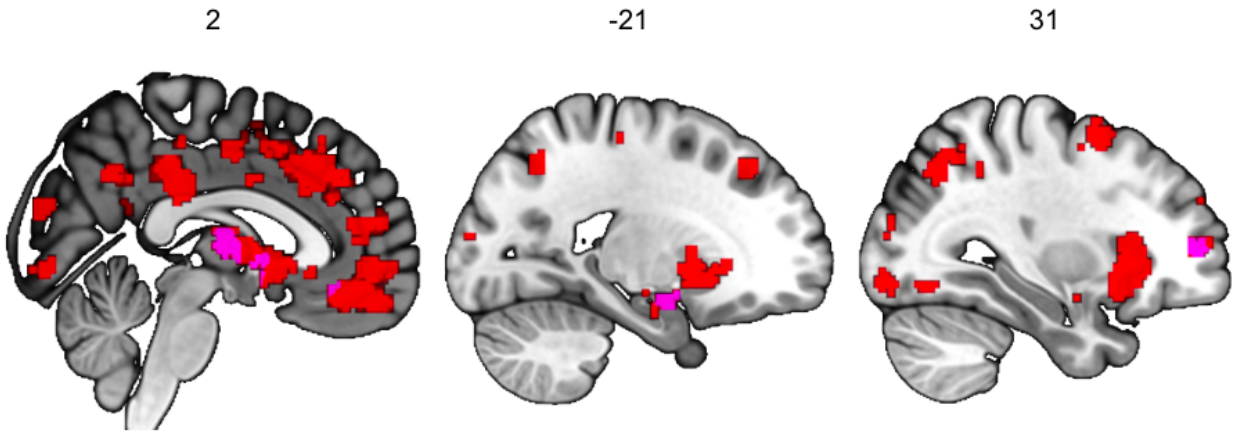

Fig S6. | Meta analysis of functional studies regarding risky behaviors (provided by Neurosynth). Depicted is the activation mask of a meta-analysis of 101 individual functional studies regarding risky behaviors (red). The conjunction with areas showing a negative association of GMV with risky behaviors is highlighted in purple, and include thalamus, vmPFC, amygdala and dlPFC (*N* = 4,717 participants, *K* = 101 individual studies, see Table S3).

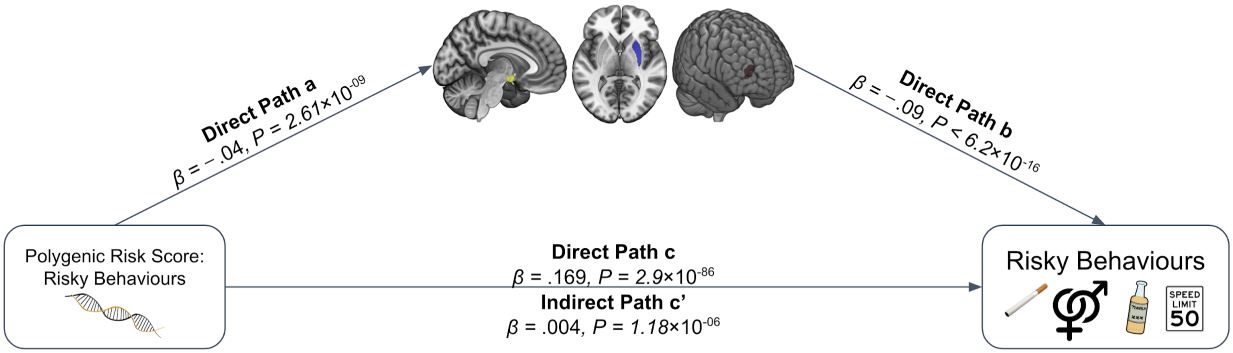

Fig S7. | Meditation analysis of the association between PRS and risky behavior with biased GMV masks. The sum of all GMV differences in right dlPFC, putamen and hypothalamus (based on the biased activation masks from Fig 2A) mediated ~2.07% of the association between the PRS and risky behavior. Arrows depict the direction of the structural equation modelling and do not imply causality.

Table S1. | Genetic correlations. We estimated genetic correlations (r_g) between risky behavior (GWAS *N* = 297,025) and 85 other traits using bivariate LD Score regression (*28*). All *P* values are two-sided.

Trait	Genetic correlation (r_g)	$SE(r_g)$	*P* value
Number of sexual partners	0.807	0.009	0.000
Smoking initiation	0.746	0.013	0.000
Ever cannabis	0.721	0.025	0.000
Drinks per week	0.698	0.016	0.000
Alcohol dependence	0.613	0.063	0.000
Maternal smoking around birth	0.581	0.026	0.000
General risk tolerance	0.559	0.021	0.000
Self-employment	0.517	0.304	0.089
Automobile speeding propensity	0.513	0.020	0.000
Suicide attempt	0.473	0.069	0.000
Antisocial behavior	0.453	0.143	0.001
Cannabis use disorder	0.442	0.097	0.000
Leisure/social activities: Pub or social club	0.433	0.028	0.000
Own or rent accommodation lived in: Own with a mortgage	0.409	0.039	0.000
Townsend deprivation index	0.401	0.046	0.000

Own or rent accommodation lived in: Rent - from private landlord or letting agency	0.350	0.073	0.000
Extraversion	0.338	0.054	0.000
Stress-related disorder	0.308	0.043	0.000
Psychiatric cross-disorder	0.256	0.036	0.000
Bipolar disorder	0.226	0.027	0.000
Major depressive disorder	0.216	0.030	0.000
Psychiatric cross-disorder	0.204	0.032	0.000
Post-traumatic stress disorder	0.198	0.052	0.000
Smoking cessation	0.190	0.033	0.000
Hip pain	0.183	0.038	0.000
Depression	0.180	0.025	0.000
Back pain	0.173	0.028	0.000
Schizophrenia	0.167	0.021	0.000
Anxiety Disorder Case-Control	0.163	0.082	0.047
Insomnia	0.149	0.027	0.000
Leisure/social activities: Sports club or gym	0.143	0.034	0.000
Knee pain	0.143	0.028	0.000
Neck or shoulder pain	0.132	0.030	0.000
Anxiety Disorder FactorScore	0.116	0.087	0.183

Cancer (diagnosed by doctor)	0.113	0.051	0.026
Cigarettes per day	0.112	0.031	0.000
Age of first facial hair (male)	0.100	0.028	0.000
Own or rent accommodation lived in: Rent - from local authority, local council, housing association	0.098	0.035	0.005
Waist-to-hip ratio (WHR)	0.089	0.019	0.000
Openness	0.076	0.060	0.206
Asthma	0.074	0.024	0.002
Coronary artery disease	0.069	0.021	0.001
Body mass index	0.066	0.019	0.001
Height	0.065	0.014	0.000
Age at menarche	0.054	0.024	0.021
Infant birth weight	0.053	0.025	0.033
Autism spectrum disorder (ASD)	0.048	0.039	0.218
Stomach or abdominal pain	0.043	0.037	0.250
Intelligence	0.039	0.023	0.093
Infant head circumference	0.036	0.061	0.557
Alzheimer's disease	0.032	0.042	0.454
Household income	0.030	0.037	0.415
Fat (diet composition)	0.009	0.038	0.825

Neuroticism	-0.012	0.059	0.834
Protein (diet composition)	-0.016	0.039	0.681
Type 2 diabetes	-0.017	0.022	0.428
Rheumatod arthritis	-0.018	0.032	0.584
Parkinson's disease	-0.022	0.054	0.693
Anorexia	-0.022	0.032	0.485
Educational attainment	-0.028	0.020	0.167
Tourette's syndrome	-0.030	0.042	0.465
Friendships satisfaction	-0.057	0.034	0.088
Leisure/social activities: Adult education class	-0.057	0.040	0.157
Blood pressure	-0.060	0.020	0.002
Childhood intelligence	-0.073	0.056	0.194
Heart rate	-0.074	0.019	0.000
Sleep duration	-0.081	0.023	0.000
Age at menopause	-0.084	0.028	0.003
Headache	-0.085	0.030	0.004
Obsessive compulsive disorder	-0.105	0.050	0.035
Subjective well-being	-0.108	0.035	0.002
Chronic kidney disease	-0.157	0.066	0.017

Chronotype	-0.162	0.022	0.000
Mother's age at death	-0.164	0.062	0.008
Parental lifespan	-0.169	0.029	0.000
Fathers age at death	-0.188	0.038	0.000
Family relationship satisfaction	-0.247	0.037	0.000
Leisure/social activities: Religious group	-0.251	0.026	0.000
Conscientiousness	-0.251	0.101	0.013
Sugar (diet composition)	-0.327	0.032	0.000
Own outright (by you or someone in your household)	-0.365	0.028	0.000
Agreeableness	-0.386	0.399	0.333
Age of smoking initiation	-0.401	0.029	0.000
Carbohydrates (diet composition)	-0.530	0.028	0.000
Age at first sex	-0.536	0.018	0.000

Table S2. | Association between risky behavior and clusters of voxels of grey matter volume (GMV). Depicted are the summarized regression statistics per voxel. ΔR^2 indicates the marginal increase in variance explained compared to a model that excludes that GMV from that cluster. The corresponding coordinates of the peak activation in each cluster can be found in Fig S3.

Cluster	β	SE	P_{uncorr}	T	R^2	ΔR^2
1	-0.1154	0.012697	1.15×10^{-19}	-9.0888	0.048208	0.006308
2	-0.10848	0.012657	1.15×10^{-17}	-8.5707	0.047519	0.005619
3	-0.063596	0.00956	3.01×10^{-11}	-6.6522	0.045312	0.003412
4	-0.061123	0.009608	2.06×10^{-10}	-6.3618	0.045026	0.003126
5	-0.077548	0.010659	3.66×10^{-13}	-7.2753	0.045969	0.004069
6	-0.071566	0.010686	2.21×10^{-11}	-6.6974	0.045358	0.003458
7	-0.054051	0.009533	1.46×10^{-08}	-5.6697	0.044394	0.002494
8	-0.065617	0.011953	4.11×10^{-08}	-5.4895	0.044242	0.002342
9	-0.065851	0.010695	7.64×10^{-10}	-6.1571	0.044832	0.002932
10	-0.064221	0.010776	2.6×10^{-09}	-5.9596	0.04465	0.00275
11	-0.066171	0.011275	4.50×10^{-09}	-5.8686	0.044569	0.002669
12	-0.060586	0.010544	9.33×10^{-09}	-5.7463	0.044461	0.002561
13	-0.056703	0.01038	4.77×10^{-08}	-5.463	0.04422	0.00232
14	-0.052643	0.009898	1.06×10^{-07}	-5.3187	0.044102	0.002202
15	-0.054197	0.010214	1.14×10^{-07}	-5.3061	0.044092	0.002192
16	-0.051553	0.010108	3.44×10^{-07}	-5.1003	0.043929	0.002029
17	-0.05134	0.010063	3.42×10^{-07}	-5.1017	0.04393	0.00203

18	-0.050687	0.009961	3.66×10^{-07}	-5.0884	0.04392	0.00202
19	-0.050047	0.010073	6.84×10^{-07}	-4.9685	0.043828	0.001928
20	-0.049129	0.009852	6.23×10^{-07}	-4.9866	0.043842	0.001942
21	-0.048736	0.010007	1.19×10^{-06}	-4.8702	0.043755	0.001855

Table S3. | List of studies used for the meta-analysis of fMRI studies on risky behaviors (provided by Neurosynth).

Title	**Author**	**Journal**	**Loading**	**Sample Size (after exclusions)**
Adolescents' Neural Processing of Risky Decisions: Effects of Sex and Behavioral Disinhibition.	Crowley TJ, Dalwani MS, Mikulich-Gilbertson SK, Young SE, Sakai JT, Raymond KM, McWilliams SK, Roark MJ, Banich MT	PloS one	0.678	81
Altered Functional Response to Risky Choice in HIV Infection.	Connolly CG, Bischoff-Grethe A, Jordan SJ, Woods SP, Ellis RJ, Paulus MP, Grant I	PloS one	0.622	40
Attenuated Neural Processing of Risk in Young Adults at Risk for Stimulant Dependence.	Reske M, Stewart JL, Flagan TM, Paulus MP	PloS one	0.576	208
Learning from other people's experience: a neuroimaging study of decisional interactive-	Canessa N, Motterlini M, Alemanno F, Perani D, Cappa SF	NeuroImage	0.564	24

learning.				
Children's brain activation during risky decision-making: A contributor to substance problems?	Crowley TJ, Dalwani MS, Sakai JT, Raymond KM, McWilliams SK, Banich MT, Mikulich-Gilbertson SK	Drug and alcohol dependence	0.52	58
Differences in neural activation as a function of risk-taking task parameters.	Congdon E, Bato AA, Schonberg T, Mumford JA, Karlsgodt KH, Sabb FW, London ED, Cannon TD, Bilder RM, Poldrack RA	Frontiers in neuroscience	0.49	23
Are risky choices actually guided by a compensatory process? New insights from FMRI.	Rao LL, Zhou Y, Xu L, Liang ZY, Jiang T, Li S	PloS one	0.442	23
Neural mechanisms of risky decision making in adolescents reporting frequent alcohol and/or marijuana use.	Claus ED, Feldstein Ewing SW, Magnan RE, Montanaro E, Hutchison KE, Bryan AD	Brain imaging and behavior	0.435	189
Neural mechanisms of impulse control in sexually risky adolescents.	Goldenberg D, Telzer EH, Lieberman MD, Fuligni A, Galvan A	Developmental cognitive neuroscience	0.429	20
Neural Mechanisms Underlying Risk and Ambiguity Attitudes.	Blankenstein NE, Peper JS, Crone EA, van	Journal of cognitive	0.414	50

	Duijvenvoorde ACK	neuroscience		
Neural correlates of expected risks and returns in risky choice across development.	van Duijvenvoorde AC, Huizenga HM, Somerville LH, Delgado MR, Powers A, Weeda WD, Casey BJ, Weber EU, Figner B	Journal of neuroscience :	0.397	72
Learning to play it safe (or not): stable and evolving neural responses during adolescent risky decision-making.	Kahn LE, Peake SJ, Dishion TJ, Stormshak EA, Pfeifer JH	Journal of cognitive neuroscience	0.392	20
Risky decisions and their consequences: neural processing by boys with Antisocial Substance Disorder.	Crowley TJ, Dalwani MS, Mikulich-Gilbertson SK, Du YP, Lejuez CW, Raymond KM, Banich MT	PloS one	0.381	40
Adolescent neural response to reward is related to participant sex and task motivation.	Alarcon G, Cservenka A, Nagel BJ	Brain and cognition	0.38	167
The neural basis of social tactics: An fMRI study.	Fukui H, Murai T, Shinozaki J, Aso T, Fukuyama H, Hayashi T, Hanakawa T	NeuroImage	0.353	16
Neural mechanisms underlying urgent and evaluative behaviors: An fMRI study on the interaction of automatic and controlled processes.	Megias A, Navas JF, Petrova D, Candido A, Maldonado A, Garcia-Retamero R, Catena A	Human brain mapping	0.348	57

Acute stress increases risky decisions and dampens prefrontal activation among adolescent boys.	Uy JP, Galvan A	NeuroImage	0.343	44
Is payoff necessarily weighted by probability when making a risky choice? Evidence from functional connectivity analysis.	Rao LL, Li S, Jiang T, Zhou Y	PloS one	0.335	18
The neural substrates of probabilistic and intertemporal decision making.	Weber BJ, Huettel SA	Brain research	0.333	23
Age-related differences in neural activities during risk taking as revealed by functional MRI.	Lee TM, Leung AW, Fox PT, Gao JH, Chan CC	Social cognitive and affective neuroscience	0.323	21
Neural mechanisms of risky decision-making and reward response in adolescent onset cannabis use disorder.	De Bellis MD, Wang L, Bergman SR, Yaxley RH, Hooper SR, Huettel SA	Drug and alcohol dependence	0.321	56
A cross-sectional and longitudinal analysis of reward-related brain activation: effects of age, pubertal stage, and reward sensitivity.	van Duijvenvoorde AC, Op de Macks ZA, Overgaauw S, Gunther Moor B, Dahl RE, Crone EA	Brain and cognition	0.319	33

Effects of outcome on the covariance between risk level and brain activity in adolescents with internet gaming disorder.	Qi X, Yang Y, Dai S, Gao P, Du X, Zhang Y, Du G, Li X, Zhang Q	NeuroImage. Clinical	0.316	48
Risky decision making and the anterior cingulate cortex in abstinent drug abusers and nonusers.	Fishbein DH, Eldreth DL, Hyde C, Matochik JA, London ED, Contoreggi C, Kurian V, Kimes AS, Breeden A, Grant S	Brain research. Cognitive brain research	0.313	27
Neural mechanisms underlying context-dependent shifts in risk preferences.	Losecaat Vermeer AB, Boksem MA, Sanfey AG	NeuroImage	0.307	26
An event-related fMRI study on risk taking by healthy individuals of high or low impulsiveness.	Lee TM, Chan CC, Han SH, Leung AW, Fox PT, Gao JH	Neuroscience letters	0.295	18
Neural responses to emotional stimuli are associated with childhood family stress.	Taylor SE, Eisenberger NI, Saxbe D, Lehman BJ, Lieberman MD	Biological psychiatry	0.291	30
Neural correlates of Machiavellian strategies in a social dilemma task.	Bereczkei T, Deak A, Papp P, Perlaki G, Orsi G	Brain and cognition	0.276	27
Sex-related differences in neural activity during risk taking: an fMRI study.	Lee TM, Chan CC, Leung AW, Fox PT, Gao JH	Cerebral cortex (New York, N.Y. :	0.272	22

		1991)		
Neurocognitive mechanisms underlying identification of environmental risks.	Qin J, Han S	Neuropsychologia	0.249	14
Neural representation of subjective value under risk and ambiguity.	Levy I, Snell J, Nelson AJ, Rustichini A, Glimcher PW	Journal of neurophysiology	0.238	29
The influence of emotion regulation on decision-making under risk.	Martin LN, Delgado MR	Journal of cognitive neuroscience	0.238	30
Failure to retreat: Blunted sensitivity to negative feedback supports risky behavior in adolescents.	McCormick EM, Telzer EH	NeuroImage	0.235	58
Pre-existing brain states predict risky choices.	Huang YF, Soon CS, Mullette-Gillman OA, Hsieh PJ	NeuroImage	0.234	14
Greater risk sensitivity of dorsolateral prefrontal cortex in young smokers than in nonsmokers.	Galvan A, Schonberg T, Mumford J, Kohno M, Poldrack RA, London ED	Psychopharmacology	0.232	43
Neuronal Correlates of Risk-Seeking Attitudes to Anticipated Losses in Binge Drinkers.	Worbe Y, Irvine M, Lange I, Kundu P, Howell NA, Harrison NA, Bullmore ET, Robbins TW, Voon V	Biological psychiatry	0.231	42

Age differences in the impact of peers on adolescents' and adults' neural response to reward.	Smith AR, Steinberg L, Strang N, Chein J	Developmental cognitive neuroscience	0.228	40
Mothers know best: redirecting adolescent reward sensitivity toward safe behavior during risk taking.	Telzer EH, Ichien NT, Qu Y	Social cognitive and affective neuroscience	0.206	25
Neural substrates of choice selection in adults and adolescents: development of the ventrolateral prefrontal and anterior cingulate cortices.	Eshel N, Nelson EE, Blair RJ, Pine DS, Ernst M	Neuropsychologia	0.202	30
The neural correlates of risk propensity in males and females using resting-state fMRI.	Zhou Y, Li S, Dunn J, Li H, Qin W, Zhu M, Rao LL, Song M, Yu C, Jiang T	Frontiers in behavioral neuroscience	0.198	289
Influence of dorsolateral prefrontal cortex and ventral striatum on risk avoidance in addiction: a mediation analysis.	Yamamoto DJ, Woo CW, Wager TD, Regner MF, Tanabe J	Drug and alcohol dependence	0.193	80
Lorazepam dose-dependently decreases risk-taking related activation in limbic areas.	Arce E, Miller DA, Feinstein JS, Stein MB, Paulus MP	Psychopharmacology	0.192	15
Neural correlates of choice	Hinvest NS, Elliott R,	Neuropsychol	0.188	34

behavior related to impulsivity and venturesomeness.	McKie S, Anderson IM	ogia		
Risk-Taking Behavior in a Computerized Driving Task: Brain Activation Correlates of Decision-Making, Outcome, and Peer Influence in Male Adolescents.	Vorobyev V, Kwon MS, Moe D, Parkkola R, Hamalainen H	PloS one	0.185	34
Risk-taking and social exclusion in adolescence: neural mechanisms underlying peer influences on decision-making.	Peake SJ, Dishion TJ, Stormshak EA, Moore WE, Pfeifer JH	NeuroImage	0.183	27
Behavioral contagion during learning about another agent's risk-preferences acts on the neural representation of decision-risk.	Suzuki S, Jensen EL, Bossaerts P, O'Doherty JP	Proceedings of the National Academy of Sciences of the United States of America	0.178	24
Functional and structural neural indices of risk aversion in obsessive-compulsive disorder (OCD).	Admon R, Bleich-Cohen M, Weizmant R, Poyurovsky M, Faragian S, Hendler T	Psychiatry research	0.175	26
Neural correlates of increased risk-taking propensity in sleep-	Lei Y, Wang L, Chen P, Li Y, Han W, Ge M, Yang L,	Brain imaging and behavior	0.17	37

deprived people along with a changing risk level.	Chen S, Hu W, Wu X, Yang Z			
Uncovering putative neural markers of risk avoidance.	Roy AK, Gotimer K, Kelly AM, Castellanos FX, Milham MP, Ernst M	Neuropsychologia	0.162	23
Buffering social influence: neural correlates of response inhibition predict driving safety in the presence of a peer.	Cascio CN, Carp J, O'Donnell MB, Tinney FJ Jr, Bingham CR, Shope JT, Ouimet MC, Pradhan AK, Simons-Morton BG, Falk EB	Journal of cognitive neuroscience	0.161	37
Neural correlates of the impact of prior outcomes on subsequent monetary decision-making in frequent poker players.	Brevers D, He Q, Xue G, Bechara A	Biological psychology	0.161	28
Decision-making under risk: an fMRI study.	Hewig J, Straube T, Trippe RH, Kretschmer N, Hecht H, Coles MG, Miltner WH	Journal of cognitive neuroscience	0.158	17
Imbalanced neural responsivity to risk and reward indicates stress vulnerability in humans.	Admon R, Lubin G, Rosenblatt JD, Stern O, Kahn I, Assaf M, Hendler T	Cerebral cortex (New York, N.Y. : 1991)	0.156	24
Neural signatures of economic parameters during decision-	Minati L, Grisoli M, Franceschetti S, Epifani F,	Brain topography	0.152	22

making: a functional MRI (FMRI), electroencephalography (EEG) and autonomic monitoring study.	Granvillano A, Medford N, Harrison NA, Piacentini S, Critchley HD			
Individual differences in risk preference predict neural responses during financial decision-making.	Engelmann JB, Tamir D	Brain research	0.151	10
Orbitofrontal reward sensitivity and impulsivity in adult attention deficit hyperactivity disorder.	Wilbertz G, van Elst LT, Delgado MR, Maier S, Feige B, Philipsen A, Blechert J	NeuroImage	0.149	56
A preliminary study of longitudinal neuroadaptation associated with recovery from addiction.	Forster SE, Finn PR, Brown JW	Drug and alcohol dependence	0.148	21
Neural correlates of anticipation risk reflect risk preferences.	Rudorf S, Preuschoff K, Weber B	Journal of neuroscience	0.147	56
Behavioral and neural correlates of loss aversion and risk avoidance in adolescents and adults.	Barkley-Levenson EE, Van Leijenhorst L, Galvan A	Developmental cognitive neuroscience	0.146	34
Dopamine agonists and risk: impulse control disorders in	Voon V, Gao J, Brezing C, Symmonds M, Ekanayake	Brain	0.142	44

Parkinson's disease.	V, Fernandez H, Dolan RJ, Hallett M			
Neural signatures of economic preferences for risk and ambiguity.	Huettel SA, Stowe CJ, Gordon EM, Warner BT, Platt ML	Neuron	0.126	13
Reduced cortical gray matter volume in male adolescents with substance and conduct problems.	Dalwani M, Sakai JT, Mikulich-Gilbertson SK, Tanabe J, Raymond K, McWilliams SK, Thompson LL, Banich MT, Crowley TJ	Drug and alcohol dependence	0.122	44
fMRI evidence for strategic decision-making during resolution of pronoun reference.	McMillan CT, Clark R, Gunawardena D, Ryant N, Grossman M	Neuropsychology	0.12	16
Entering adolescence: resistance to peer influence, risky behavior, and neural changes in emotion reactivity.	Pfeifer JH, Masten CL, Moore WE 3rd, Oswald TM, Mazziotta JC, Iacoboni M, Dapretto M	Neuron	0.118	38
The neural basis of financial risk taking.	Kuhnen CM, Knutson B	Neuron	0.116	19
Variables influencing the neural correlates of perceived risk of physical harm.	Coaster M, Rogers BP, Jones OD, Viscusi WK, Merkle KL, Zald DH, Gore JC	Cognitive, affective & behavioral neuroscience	0.116	19

Distinct encoding of risk and value in economic choice between multiple risky options.	Wright ND, Symmonds M, Dolan RJ	NeuroImage	0.113	24
Decreasing ventromedial prefrontal cortex deactivation in risky decision making after simulated microgravity: effects of -6 degrees head-down tilt bed rest.	Rao LL, Zhou Y, Liang ZY, Rao H, Zheng R, Sun Y, Tan C, Xiao Y, Tian ZQ, Chen XP, Wang CH, Bai YQ, Chen SG, Li S	Frontiers in behavioral neuroscience	0.112	16
Adolescent neurodevelopment of cognitive control and risk-taking in negative family contexts.	McCormick EM, Qu Y, Telzer EH	NeuroImage	0.11	20
Individual differences in risk-taking tendencies modulate the neural processing of risky and ambiguous decision-making in adolescence.	Blankenstein NE, Schreuders E, Peper JS, Crone EA, van Duijvenvoorde ACK	NeuroImage	0.106	198
Morphometric correlation of impulsivity in medial prefrontal cortex.	Cho SS, Pellecchia G, Aminian K, Ray N, Segura B, Obeso I, Strafella AP	Brain topography	0.104	34
Processing of decision-making and social threat in patients with history of suicidal attempt: A neuroimaging replication study.	Olie E, Ding Y, Le Bars E, de Champfleur NM, Mura T, Bonafe A, Courtet P, Jollant F	Psychiatry research	0.102	73

Sleep deprivation is associated with attenuated parametric valuation and control signals in the midbrain during value-based decision making.	Menz MM, Buchel C, Peters J	Journal of neuroscience	0.101	22
Adaptive Adolescent Flexibility: Neurodevelopment of Decision-making and Learning in a Risky Context.	McCormick EM, Telzer EH	Journal of cognitive neuroscience	0.1	77
Decreased activation of lateral orbitofrontal cortex during risky choices under uncertainty is associated with disadvantageous decision-making and suicidal behavior.	Jollant F, Lawrence NS, Olie E, O'Daly O, Malafosse A, Courtet P, Phillips ML	NeuroImage	0.096	40
Nothing to lose: processing blindness to potential losses drives thrill and adventure seekers.	Kruschwitz JD, Simmons AN, Flagan T, Paulus MP	NeuroImage	0.096	188
How the risky features of previous selection affect subsequent decision-making: evidence from behavioral and fMRI measures.	Dong G, Zhang Y, Xu J, Lin X, Du X	Frontiers in neuroscience	0.094	22
Individualized relapse prediction: Personality	Gowin JL, Ball TM, Wittmann M, Tapert SF,	Drug and alcohol	0.09	68

measures and striatal and insular activity during reward-processing robustly predict relapse.	Paulus MP	dependence		
Reduced posterior mesofrontal cortex activation by risky rewards in substance-dependent patients.	Bjork JM, Momenan R, Smith AR, Hommer DW	Drug and alcohol dependence	0.089	34
Neural prediction errors reveal a risk-sensitive reinforcement-learning process in the human brain.	Niv Y, Edlund JA, Dayan P, O'Doherty JP	Journal of neuroscience	0.089	16
Increased activation in the right insula during risk-taking decision making is related to harm avoidance and neuroticism.	Paulus MP, Rogalsky C, Simmons A, Feinstein JS, Stein MB	NeuroImage	0.087	17
Neural activities underlying environmental and personal risk identification tasks.	Qin J, Lee TM, Wang F, Mao L, Han S	Neuroscience letters	0.086	14
The Effect of Wealth Shocks on Loss Aversion: Behavior and Neural Correlates.	Pammi VSC, Ruiz S, Lee S, Noussair CN, Sitaram R	Frontiers in neuroscience	0.086	15
The functional and structural neural basis of individual differences in loss aversion.	Canessa N, Crespi C, Motterlini M, Baud-Bovy G, Chierchia G, Pantaleo	Journal of neuroscience	0.085	56

	G, Tettamanti M, Cappa SF			
Developmental continuity in reward-related enhancement of cognitive control.	Strang NM, Pollak SD	Developmental cognitive neuroscience	0.085	65
Aberrant neural signatures of decision-making: Pathological gamblers display cortico-striatal hypersensitivity to extreme gambles.	Gelskov SV, Madsen KH, Ramsoy TZ, Siebner HR	NeuroImage	0.085	29
Neural activity associated with the passive prediction of ambiguity and risk for aversive events.	Bach DR, Seymour B, Dolan RJ	Journal of neuroscience	0.084	20
Gender differences in reward-related decision processing under stress.	Lighthall NR, Sakaki M, Vasunilashorn S, Nga L, Somayajula S, Chen EY, Samii N, Mather M	Social cognitive and affective neuroscience	0.083	47
Parsing neural mechanisms of social and physical risk identifications.	Qin J, Han S	Human brain mapping	0.082	14
Too little, too late or too much, too early? Differential hemodynamics of response inhibition in high and low sensation seekers	Collins HR, Corbly CR, Liu X, Kelly TH, Lynam D, Joseph JE	Brain research	0.082	40

Stress and decision making: neural correlates of the interaction between stress, executive functions, and decision making under risk.	Gathmann B, Schulte FP, Maderwald S, Pawlikowski M, Starcke K, Schafer LC, Scholer T, Wolf OT, Brand M	Experimental brain research	0.08	33
Comparing apples and oranges: using reward-specific and reward-general subjective value representation in the brain.	Levy DJ, Glimcher PW	Journal of neuroscience	0.077	19
The effect of age on neural processing of pleasant soft touch stimuli.	May AC, Stewart JL, Tapert SF, Paulus MP	Frontiers in behavioral neuroscience	0.076	58
Reduced functional connectivity of fronto-parietal sustained attention networks in severe childhood abuse.	Hart H, Lim L, Mehta MA, Chatzieffraimidou A, Curtis C, Xu X, Breen G, Simmons A, Mirza K, Rubia K	PloS one	0.076	48
Neural sensitivity to absolute and relative anticipated reward in adolescents.	Vaidya JG, Knutson B, O'Leary DS, Block RI, Magnotta V	PloS one	0.075	36
Serotonin 2A receptors contribute to the regulation of risk-averse decisions.	Macoveanu J, Rowe JB, Hornboll B, Elliott R, Paulson OB, Knudsen GM, Siebner HR	NeuroImage	0.075	20

Neural correlates of stress and favorite-food cue exposure in adolescents: a functional magnetic resonance imaging study.	Hommer RE, Seo D, Lacadie CM, Chaplin TM, Mayes LC, Sinha R, Potenza MN	Human brain mapping	0.067	43
The neural basis of social risky decision making in females with major depressive disorder.	Shao R, Zhang HJ, Lee TM	Neuropsychologia	0.067	29
Neural substrates of reward magnitude, probability, and risk during a wheel of fortune decision-making task.	Smith BW, Mitchell DG, Hardin MG, Jazbec S, Fridberg D, Blair RJ, Ernst M	NeuroImage	0.064	25
Heightened activity in social reward networks is associated with adolescents' risky sexual behaviors.	Eckstrand KL, Choukas-Bradley S, Mohanty A, Cross M, Allen NB, Silk JS, Jones NP, Forbes EE	Developmental cognitive neuroscience	0.059	47
Neural correlates of high-risk behavior tendencies and impulsivity in an emotional Go/NoGo fMRI task.	Brown MR, Benoit JR, Juhas M, Lebel RM, MacKay M, Dametto E, Silverstone PH, Dolcos F, Dursun SM, Greenshaw AJ	Frontiers in systems neuroscience	0.054	19

Supplementary References

1. K. L. Miller, F. Alfaro-Almagro, N. K. Bangerter, D. L. Thomas, E. Yacoub, J. Xu, A. J. Bartsch, S. Jbabdi, S. N. Sotiropoulos, J. L. R. Andersson, L. Griffanti, G. Douaud, T. W. Okell, P. Weale, I. Dragonu, S. Garratt, S. Hudson, R. Collins, M. Jenkinson, P. M. Matthews, S. M. Smith, Multimodal population brain imaging in the UK Biobank prospective epidemiological study. *Nature Neuroscience*. **19** (2016), pp. 1523–1536.

2. C. Sudlow, J. Gallacher, N. Allen, V. Beral, P. Burton, J. Danesh, P. Downey, P. Elliott, J. Green, M. Landray, B. Liu, P. Matthews, G. Ong, J. Pell, A. Silman, A. Young, T. Sprosen, T. Peakman, R. Collins, UK biobank: an open access resource for identifying the causes of a wide range of complex diseases of middle and old age. *PLoS Med.* **12**, e1001779 (2015).

3. G. Nave, W. H. Jung, R. Karlsson Linnér, J. W. Kable, P. D. Koellinger, Are Bigger Brains Smarter? Evidence From a Large-Scale Preregistered Study. *Psychol. Sci.*, 956797618808470 (2018).

4. C. Harper, The neurotoxicity of alcohol. *Hum. Exp. Toxicol.* **26**, 251–257 (2007).

5. H. R. Kranzler, R. Wetherill, R. Feinn, T. Pond, J. Gelernter, J. Covault, Posttreatment effects of topiramate treatment for heavy drinking. *Alcohol. Clin. Exp. Res.* **38**, 3017–3023 (2014).

6. F. Alfaro-Almagro, M. Jenkinson, N. K. Bangerter, J. L. R. Andersson, L. Griffanti, G. Douaud, S. N. Sotiropoulos, S. Jbabdi, M. Hernandez-Fernandez, E. Vallee, D. Vidaurre, M. Webster, P. McCarthy, C. Rorden, A. Daducci, D. C. Alexander, H. Zhang, I. Dragonu, P. M. Matthews, K. L. Miller, S. M. Smith, Image processing and Quality Control for the first 10,000 brain imaging datasets from UK Biobank. *Neuroimage*. **166**, 400–424 (2018).

7. R. Karlsson Linnér, P. Biroli, E. Kong, S. F. W. Meddens, R. Wedow, M. A. Fontana, M. Lebreton, S. P. Tino, A. Abdellaoui, A. R. Hammerschlag, M. G. Nivard, A. Okbay, C. A. Rietveld, P. N. Timshel, M. Trzaskowski, R. de Vlaming, C. L. Zünd, Y. Bao, L. Buzdugan, A. H. Caplin, C.-Y. Chen, P. Eibich, P. Fontanillas, J. R. Gonzalez, P. K. Joshi, V. Karhunen, A. Kleinman, R. Z. Levin, C. M. Lill, G. A. Meddens, G. Muntané, S. Sanchez-Roige, F. J. van Rooij, E. Taskesen, Y. Wu, F. Zhang, 23and Me Research Team, eQTLgen Consortium, International Cannabis Consortium, Social Science Genetic Association Consortium, A. Auton, J. D. Boardman, D. W. Clark, A. Conlin, C. C. Dolan, U. Fischbacher, P. J. F. Groenen, K. M. Harris, G. Hasler, A. Hofman, M. A. Ikram, S. Jain, R. Karlsson, R. C. Kessler, M. Kooyman, J. MacKillop, M. Männikkö, C. Morcillo-Suarez, M. B. McQueen, K. M. Schmidt, M. C. Smart, M. Sutter, A. R. Thurik, A. G. Uitterlinden, J. White, H. de Wit, J. Yang, L. Bertram, D. I. Boomsma, T. Esko, E. Fehr, D. A. Hinds, M. Johannesson, M. Kumari, D. Laibson, P. K. E. Magnusson, M. N. Meyer, A. Navarro, A. A. Palmer, T. H. Pers, D. Posthuma, D. Schunk, M. B. Stein, R. Svento, H. Tiemeier, P. R. H. J. Timmers, P. Turley, R. J. Ursano, G. G. Wagner, J. F. Wilson, J. Gratten, J. J. Lee, D. Cesarini, D. J. Benjamin, P. D. Koellinger, J. P.

Beauchamp, Genome-wide association analyses of risk tolerance and risky behaviors in over 1 million individuals identify hundreds of loci and shared genetic influences. *Nat. Genet.* **51**, 245–257 (2019).

8. L. L. Desiderato, H. J. Crawford, Risky sexual behavior in college students: Relationships between number of sexual partners, disclosure of previous risky behavior, and alcohol use. *Journal of Youth and Adolescence*. **24** (1995), pp. 55–68.

9. R. Mata, R. Frey, D. Richter, J. Schupp, R. Hertwig, Risk Preference: A View from Psychology. *J. Econ. Perspect.* **32**, 155–172 (2018).

10. R. Mata, A. K. Josef, R. Hertwig, Propensity for Risk Taking Across the Life Span and Around the Globe. *Psychol. Sci.* **27**, 231–243 (2016).

11. J.-E. Lönnqvist, M. Verkasalo, G. Walkowitz, P. C. Wichardt, Measuring individual risk attitudes in the lab: Task or ask? An empirical comparison. *Journal of Economic Behavior & Organization*. **119** (2015), pp. 254–266.

12. R. Croson, U. Gneezy, Gender Differences in Preferences. *J. Econ. Lit.* **47**, 448–474 (2009).

13. T. Dohmen, A. Falk, D. Huffman, U. Sunde, J. Schupp, G. G. Wagner, INDIVIDUAL RISK ATTITUDES: MEASUREMENT, DETERMINANTS, AND BEHAVIORAL CONSEQUENCES. *Journal of the European Economic Association*. **9** (2011), pp. 522–550.

14. L. R. Cardon, L. J. Palmer, Population stratification and spurious allelic association. *Lancet*. **361**, 598–604 (2003).

15. J. Sallet, R. B. Mars, M. P. Noonan, F.-X. Neubert, S. Jbabdi, J. X. O'Reilly, N. Filippini, A. G. Thomas, M. F. Rushworth, The organization of dorsal frontal cortex in humans and macaques. *J. Neurosci.* **33**, 12255–12274 (2013).

16. F.-X. Neubert, R. B. Mars, J. Sallet, M. F. S. Rushworth, Connectivity reveals relationship of brain areas for reward-guided learning and decision making in human and monkey frontal cortex. *Proc. Natl. Acad. Sci. U. S. A.* **112**, E2695–704 (2015).

17. E. D. Boorman, T. E. J. Behrens, M. W. Woolrich, M. F. S. Rushworth, How Green Is the Grass on the Other Side? Frontopolar Cortex and the Evidence in Favor of Alternative Courses of Action. *Neuron*. **62** (2009), pp. 733–743.

18. S.-L. Lim, S. -L. Lim, J. P. O'Doherty, A. Rangel, The Decision Value Computations in the vmPFC and Striatum Use a Relative Value Code That is Guided by Visual Attention. *Journal of Neuroscience*. **31** (2011), pp. 13214–13223.

19. H. C. Barron, R. J. Dolan, T. E. J. Behrens, Online evaluation of novel choices by simultaneous representation of multiple memories. *Nature Neuroscience*. **16** (2013), pp. 1492–1498.

20. J. W. Kable, P. W. Glimcher, The neural correlates of subjective value during intertemporal choice. *Nat. Neurosci.* **10**, 1625 (2007).

21. D. Ongur, The Organization of Networks within the Orbital and Medial Prefrontal Cortex of Rats, Monkeys and Humans. *Cerebral Cortex*. **10** (2000), pp. 206–219.

22. W. M. Pauli, A. N. Nili, J. M. Tyszka, A high-resolution probabilistic in vivo atlas of human subcortical brain nuclei. *Sci Data*. **5**, 180063 (2018).

23. J. Poppenk, H. R. Evensmoen, M. Moscovitch, L. Nadel, Long-axis specialization of the human hippocampus. *Trends Cogn. Sci.* **17**, 230–240 (2013).

24. L. J. Chang, T. Yarkoni, M. W. Khaw, A. G. Sanfey, Decoding the role of the insula in human cognition: functional parcellation and large-scale reverse inference. *Cereb. Cortex*. **23**, 739–749 (2013).

25. A. Manichaikul, J. C. Mychaleckyj, S. S. Rich, K. Daly, M. Sale, W.-M. Chen, Robust relationship inference in genome-wide association studies. *Bioinformatics*. **26**, 2867–2873 (2010).

26. P.-R. Loh, G. Tucker, B. K. Bulik-Sullivan, B. J. Vilhjálmsson, H. K. Finucane, R. M. Salem, D. I. Chasman, P. M. Ridker, B. M. Neale, B. Berger, N. Patterson, A. L. Price, Efficient Bayesian mixed-model analysis increases association power in large cohorts. *Nat. Genet.* **47**, 284–290 (2015).

27. P.-R. Loh, G. Kichaev, S. Gazal, A. P. Schoech, A. L. Price, Mixed-model association for biobank-scale datasets. *Nat. Genet.* **50**, 906–908 (2018).

28. B. K. Bulik-Sullivan, H. K. Finucane, V. Anttila, A. Gusev, F. R. Day, R. Consortium, P. Genomics Consortium, G. C. F. A. of the Wellcome Trust Consortium, J. R. B. B. Perry, N. Patterson, E. B. Robinson, M. J. Daly, A. L. Price, B. M. Neale, ReproGen Consortium, G. C. F. A. Psychiatric Genomics Consortium of the Wellcome Trust Consortium, P.-R. Loh, L. Duncan, An atlas of genetic correlations across human diseases and traits. *Nat. Genet.* **47**, 1236–1241 (2015).

29. K. Watanabe, S. Stringer, O. Frei, M. Umićević Mirkov, C. de Leeuw, T. J. C. Polderman, S. van der Sluis, O. A. Andreassen, B. M. Neale, D. Posthuma, A global overview of pleiotropy and genetic architecture in complex traits. *Nat. Genet.* (2019), doi:10.1038/s41588-019-0481-0.

30. S. F. W. Meddens, R. de Vlaming, P. Bowers, C. A. P. Burik, R. K. Linnér, C. Lee, A. Okbay, P. Turley, C. A. Rietveld, M. A. Fontana, M. Ghanbari, F. Imamura, G. McMahon, P. J. van der Most, V. Trudy, K. H. Wade, E. L. Anderson, K. V. E. Braun, P. M. Emmett, T. Esko, J. R. Gonzalez, J. C. Kiefte-de Jong, J. Luan, C. Langenberg, T. Muka, S. Ring, F. Rivadeneira, J. D. Schoufour, H. Snieder, F. J. A. van Rooij, B. H. R. Wolffenbuttel, G. D. Smith, O. H. Franco, N. G. Forouhi, M. Arfan Ikram, A. G. Uitterlinden, J. V. van Vliet-Ostaptchouk, N. J. Wareham, D. Cesarini, K. Paige Harden, J. J. Lee, D. J. Benjamin, C. C. Chow, P. D. Koellinger, 23andMe Research Team, EPIC-InterAct Consortium, Lifelines Cohort Study, Genomic analysis of diet composition finds novel loci and associations with health

and lifestyle, , doi:10.1101/383406.

31. International HapMap 3 Consortium, D. M. Altshuler, R. A. Gibbs, L. Peltonen, D. M. Altshuler, R. A. Gibbs, L. Peltonen, E. Dermitzakis, S. F. Schaffner, F. Yu, L. Peltonen, E. Dermitzakis, P. E. Bonnen, D. M. Altshuler, R. A. Gibbs, P. I. W. de Bakker, P. Deloukas, S. B. Gabriel, R. Gwilliam, S. Hunt, M. Inouye, X. Jia, A. Palotie, M. Parkin, P. Whittaker, F. Yu, K. Chang, A. Hawes, L. R. Lewis, Y. Ren, D. Wheeler, R. A. Gibbs, D. M. Muzny, C. Barnes, K. Darvishi, M. Hurles, J. M. Korn, K. Kristiansson, C. Lee, S. A. McCarrol, J. Nemesh, E. Dermitzakis, A. Keinan, S. B. Montgomery, S. Pollack, A. L. Price, N. Soranzo, P. E. Bonnen, R. A. Gibbs, C. Gonzaga-Jauregui, A. Keinan, A. L. Price, F. Yu, V. Anttila, W. Brodeur, M. J. Daly, S. Leslie, G. McVean, L. Moutsianas, H. Nguyen, S. F. Schaffner, Q. Zhang, M. J. R. Ghori, R. McGinnis, W. McLaren, S. Pollack, A. L. Price, S. F. Schaffner, F. Takeuchi, S. R. Grossman, I. Shlyakhter, E. B. Hostetter, P. C. Sabeti, C. A. Adebamowo, M. W. Foster, D. R. Gordon, J. Licinio, M. C. Manca, P. A. Marshall, I. Matsuda, D. Ngare, V. O. Wang, D. Reddy, C. N. Rotimi, C. D. Royal, R. R. Sharp, C. Zeng, L. D. Brooks, J. E. McEwen, Integrating common and rare genetic variation in diverse human populations. *Nature*. **467**, 52–58 (2010).

32. J. Ashburner, K. J. Friston, Voxel-Based Morphometry—The Methods. *Neuroimage*. **11**, 805–821 (2000).

33. T. Yarkoni, R. A. Poldrack, T. E. Nichols, D. C. Van Essen, T. D. Wager, Large-scale automated synthesis of human functional neuroimaging data. *Nat. Methods*. **8**, 665–670 (2011).

34. D. A. Dickie, S. Mikhael, D. E. Job, J. M. Wardlaw, D. H. Laidlaw, M. E. Bastin, Permutation and parametric tests for effect sizes in voxel-based morphometry of gray matter volume in brain structural MRI. *Magnetic Resonance Imaging*. **33** (2015), pp. 1299–1305.

35. M. M. Owens, J. C. Gray, M. T. Amlung, A. Oshri, L. H. Sweet, J. MacKillop, Neuroanatomical foundations of delayed reward discounting decision making. *NeuroImage*. **161** (2017), pp. 261–270.

36. W. H. Jung, S. Lee, C. Lerman, J. W. Kable, Amygdala Functional and Structural Connectivity Predicts Individual Risk Tolerance. *Neuron*. **98** (2018), pp. 394–404.e4.

37. D. J. Hagler Jr, S. Hatton, M. D. Cornejo, C. Makowski, D. A. Fair, A. S. Dick, M. T. Sutherland, B. J. Casey, D. M. Barch, M. P. Harms, R. Watts, J. M. Bjork, H. P. Garavan, L. Hilmer, C. J. Pung, C. S. Sicat, J. Kuperman, H. Bartsch, F. Xue, M. M. Heitzeg, A. R. Laird, T. T. Trinh, R. Gonzalez, S. F. Tapert, M. C. Riedel, L. M. Squeglia, L. W. Hyde, M. D. Rosenberg, E. A. Earl, K. D. Howlett, F. C. Baker, M. Soules, J. Diaz, O. R. de Leon, W. K. Thompson, M. C. Neale, M. Herting, E. R. Sowell, R. P. Alvarez, S. W. Hawes, M. Sanchez, J. Bodurka, F. J. Breslin, A. S. Morris, M. P. Paulus, W. K. Simmons, J. R. Polimeni, A. van der Kouwe, A. S. Nencka, K. M. Gray, C. Pierpaoli, J. A. Matochik, A. Noronha, W. M. Aklin, K. Conway, M. Glantz, E. Hoffman, R. Little, M. Lopez, V. Pariyadath, S. R. Weiss, D.

L. Wolff-Hughes, R. DelCarmen-Wiggins, S. W. Feldstein Ewing, O. Miranda-Dominguez, B. J. Nagel, A. J. Perrone, D. T. Sturgeon, A. Goldstone, A. Pfefferbaum, K. M. Pohl, D. Prouty, K. Uban, S. Y. Bookheimer, M. Dapretto, A. Galvan, K. Bagot, J. Giedd, M. A. Infante, J. Jacobus, K. Patrick, P. D. Shilling, R. Desikan, Y. Li, L. Sugrue, M. T. Banich, N. Friedman, J. K. Hewitt, C. Hopfer, J. Sakai, J. Tanabe, L. B. Cottler, S. J. Nixon, L. Chang, C. Cloak, T. Ernst, G. Reeves, D. N. Kennedy, S. Heeringa, S. Peltier, J. Schulenberg, C. Sripada, R. A. Zucker, W. G. Iacono, M. Luciana, F. J. Calabro, D. B. Clark, D. A. Lewis, B. Luna, C. Schirda, T. Brima, J. J. Foxe, E. G. Freedman, D. W. Mruzek, M. J. Mason, R. Huber, E. McGlade, A. Prescot, P. F. Renshaw, D. A. Yurgelun-Todd, N. A. Allgaier, J. A. Dumas, M. Ivanova, A. Potter, P. Florsheim, C. Larson, K. Lisdahl, M. E. Charness, B. Fuemmeler, J. M. Hettema, H. H. Maes, J. Steinberg, A. P. Anokhin, P. Glaser, A. C. Heath, P. A. Madden, A. Baskin-Sommers, R. T. Constable, S. J. Grant, G. J. Dowling, S. A. Brown, T. L. Jernigan, A. M. Dale, Image processing and analysis methods for the Adolescent Brain Cognitive Development Study. *Neuroimage*. **202**, 116091 (2019).

38. S. R. Cox, S. J. Ritchie, C. Fawns-Ritchie, E. M. Tucker-Drob, I. J. Deary, Brain imaging correlates of general intelligence in UK Biobank. *bioRxiv* (2019), p. 599472.